REACTION OF SIMPLE ORGANIC ACID WITH CALCITE: EFFECT OF REVERSIBLE REACTIONS

A Thesis

by

ABHISHEK PUNASE

Submitted to the Office of Graduate and Professional Studies of
Texas A&M University
in partial fulfillment of the requirements for the degree of

MASTER OF SCIENCE

Chair of Committee,	Hisham Nasr-El-Din
Committee Members,	Jerome Schubert
	Mahmoud El-Halwagi
Head of Department,	Daniel A. Hill

May 2015

Major Subject: Petroleum Engineering

Copyright 2015 Abhishek Punase

ABSTRACT

Matrix acidizing is widely-used in the petroleum industry as a production enhancement technique. In order to design a successful acidizing job, it is important that all aspects of the reaction between the treating acid and the formation rock are understood. The reaction-rate studies involving organic acids seem to present conflicting results regarding the influence of reversible reactions. The primary objective of this paper is to comprehensively investigate the effects of the backward reactions on the kinetics of the acidizing process.

In order to understand how weak acids influence the reaction process, a comparative study of the different mathematical models existing in the literature was conducted and its results have been included in this work. Moreover, experimental data were also generated by carrying out experiments with acetic acid on calcite marble disks at different temperatures (80, 150, 200, and 250°F), acid concentrations (0.5, 1.0, 1.5, and 2.0 molar), and disk rotational speeds (100 - 1700 RPM) using a rotating disk apparatus.

These studies suggest that the rock porosity and backward reactions can significantly affect the rate of reaction and should not be neglected. For acidizing processes involving weak organic acids (such as acetic acid, formic acid, lactic acid, etc.), it was observed that the dissolution rates estimated by the different models gave distinct results and varied in two order of magnitudes from each other. This large variation can be attributed to the fact that the rate determination process by one method

account for the concentration of all the interfacial ions generated during the reversible reactions, whereas the other approach considers only the presence hydrogen ions as a rate affecting parameter.

The inclusion of reversible reaction effects on the kinetics study can improve the accuracy up to 55-60%. Therefore, evaluation of all these aspects can lead us to develop a better field approach intended for the use of weak organic acids for well stimulation jobs. It also emphasizes that strong and weak acid systems have very different surface reaction mechanisms and, therefore, their kinetics cannot be estimated in the same manner.

ACKNOWLEDGEMENTS

I would like to thank my committee chair, Dr. Nasr-El-Din, for his guidance and for providing me with the opportunity to further my education and learning. I would also like to thank Dr. Schubert and Dr. El-Halwagi for serving on my committee.

My friends and colleagues also deserve thanks for their constant encouragement during the course of my research and for making my time at Texas A&M University an enjoyable one.

Finally, I would like to extend my gratitude to my parents, sister and entire family for their constant support and faith in me.

NOMENCLATURE

C_b	Bulk concentration
C_s	Interfacial concentration
CI	Corrosion Inhibitor
CO_2	Carbon dioxide
D	Diffusion coefficient
E_a	Activation energy
HAc	Acetic acid
HCl	Hydrochloric acid
I	Ionic strength
ICP-OES	Inductively coupled plasma – Optical emission spectroscopy
K_c	Conditional equilibrium constant
K_{eff}	Effective equilibrium constant
K_{MT}	Mass transfer coefficient
k_r	Effective surface reaction rate constant
n	Reaction order
N	Acid molality
r_D	Dissolution rate
R	Universal gas constant
RDA	Rotating disk apparatus
S_c	Schmidt number

T	Temperature
z	Ionic charge
γ	Activity coefficient
κ	Overall reaction rate constant
ν	Kinematic viscosity
μ	Dynamic viscosity
ρ	Density
ω	Disk rotational speed

TABLE OF CONTENTS

Page

LIST OF FIGURES

Page

LIST OF TABLES

Page

CHAPTER I

INTRODUCTION AND LITERATURE REVIEW

A reservoir is a heterogeneous system consisting of different fluids and rock minerals. The physical and chemical interactions between these two phases can often damage the formation by plugging the pores and blocking the flow channels. In such cases, well stimulation techniques like matrix acidizing and acid fracturing can be used to improve the reservoir permeability.

Formation damage can be caused due to several mechanisms like incompatibilities between rock-fluid or injected fluid-reservoir fluid systems, fines migration, wettability alteration, phase trapping, solid invasion, etc. Even the production of polysaccharide slimes as biological waste by microbes can damage the near well bore region of the formation (Bennion, and Thomas 1994).

Matrix acidizing works on the principle of the chemical reactions that takes place between the rock minerals and the injected acid solution. If the acid can dissolve either the rock matrix or the minerals damaging the near well bore region, then it can create the channels (wormholes) through which the crude can migrate. During an acidizing process, the acid injection pressure is maintained lower than the formation fracture pressure. The first on-field acidizing treatment was conducted by Standard Oil Company in 1896, where carbonate formation in Lima, Ohio was stimulated using concentrated hydrochloric acid (Kalfayan 2008).

HCl is one of the most commonly used stimulation fluid in the industry. The main advantage of HCl is that it is a strong acid, so it can dissociate quickly and rapidly react with the formation. It is also inexpensive and easily available. Moreover, the products generated by the reaction of calcite and HCl are water soluble and hence no issues related to re-precipitation are observed (Williams, Gidley, and Schechter 1979).

While operating in deeper formations, where the bottom-hole temperature is very high, reaction of HCl becomes very rapid. The high reaction rate results in face or complete dissolution of the carbonate minerals, which does not yield high conductivity enhancement and also consumes large volume of the injected acid (Fredd, and Fogler 1998). Weak formations can even collapse due to the rapid spending of such strong acids like HCl. Another important disadvantage of using HCl at higher temperature condition is its high corrosive tendency which can severely damage the wellbore equipment (Schechter 1992).

Additives like corrosion inhibitors (CI) are added to the acid solution before injecting it in order to lower the corrosion impact. The CI generally forms a film at the tubular surface and prevents the direct interaction between the acid and the metal. Study conducted by Schauhoff and Kissel (2000) suggests that most of the effective CI films are made up of amines or their salts which start to decompose at temperatures above 482°F, so the thermal stability of these chemicals needs to be studied. Moreover, corrosion inhibitors can get adsorbed at the reservoir rock surface and alter its wettability resulting in lower dissolution (Crowe, and Minor 1982). Another possible problem is the

fluid-fluid incompatibility that can arise between CI and other additives of the stimulation fluid.

Organic acids such as formic and acetic acid possess distinct advantage over HCl at high temperature conditions due to their slow spending rate (Nierode, and Williams 1971). This allows the acid to penetrate through the formation easily and improve its conductivity. The corrosive capacity and sludge formation tendency of organic acids is also lower than HCl.

Although formic acid is known to be the strongest organic acid with dissociation constant of 1.8×10^{-4} mol/L, but its use as a stand-alone stimulation fluid is limited. This is because of the low solubility of calcium formate at higher concentrations (above 10%) of formic acid (Kalfayan 2008). Calcium acetate, on the other hand has better solubility at higher concentrations of acetic acid. Furthermore, study conducted by Harris (1961) points out that the corrosion caused by acetic acid and HCl differ with each other, the former acid follows a uniform removal of steel pattern whereas the latter develops pit corrosion. Pit corrosion causes the serious damage to the wellbore equipment and reduces its life. All these advantages make acetic acid a good alternative to HCl as an acidizing fluid. Apart from stand-alone stimulation fluid, acetic acid has been used in various other oilfield applications as perforating fluid, emulsified acid with formic and hydrochloric acid, kill fluid, etc.

The overall reaction between an acid solution and a reactive rock involves the following three processes:

a. Transport of reactant from the bulk solution to the rock surface.

b. Surface reaction between H^+ and rock minerals

c. Transport of reaction product away from the surface

The slowest step among the three limits the overall reaction rate (Rozieres, Chang, and Sullivan 1994). If steps a or step c is the slowest step, then the reaction is called as mass transfer limiting or else it is called as a surface reaction limiting reaction. Each of the three steps affects the overall reaction system differently and therefore it is important to study these processes independently.

The success of an acidizing job depends on selecting the correct type, concentration and injection rate of the acid. An acidizing process can either be a mass transfer or a surface reaction limiting depending on its reaction kinetics and injection rate values. In order to design an optimum acid treatment, it is very important to comprehend the limiting regime of the process.

Calcite dissolution studies have been expansively conducted throughout the acidic medium (pH range from 0 to 7) by various researchers (Lund et al. 1975; Sjöberg, and Rickard 1984; Nierode, and Williams 1971; Lund, Fogler, and McCune 1973; Pokrovsky, Golubev, and Schott 2005). Depending on the pH conditions and the partial pressure exerted by the released CO_2, it was observed that the carbonate minerals can undergo three surface reactions simultaneously:

$$H^+ + CaCO_3 \rightleftharpoons Ca^{2+} + HCO_3^- \quad \text{Eq. 1.1}$$

$$H_2CO_3 + CaCO_3 \rightleftharpoons Ca^{2+} + 2HCO_3^- \quad \text{Eq. 1.2}$$

$$H_2O + CaCO_3 \rightleftharpoons Ca^{2+} + HCO_3^- + OH^- \quad \text{Eq. 1.3}$$

The reaction between carbonate and carbonic acid (Eq. 1.2) becomes important when the CO_2 partial pressure is greater than 0.1 atm and higher pH values (above 5). In case of lower partial pressure of CO_2, the carbonate reaction is dominated by H^+ (Eq. 1.1) at low pH while H_2O reaction (Eq. 1.3) becomes significant at higher pH condition (Plummer, Wigley, and Parkhurst 1978).

A detailed analysis and a comparative study of currently existing models for both mass transfer as well as surface reaction limited regime of acetic acid reaction with carbonate rock is included in this study. Experimental analyses were also carried to comprehend how different parameters like acid concentration, temperature, and rotational speed can alter the reaction kinetics. The results were used to analyze the appropriateness and accuracy of various analytical models at different conditions.

CHAPTER II

THEORETICAL MODEL

As stated in chapter I, the kinetics of calcite dissolution with HCl has been well studied and documented. Many of the commercially used acidizing software packages are developed based on the HCl/calcite reaction system. The same is not the case with organic acids, primarily because of the complexities associated with its incomplete dissociation and occurrence of reversible reactions. Both these phenomenon greatly affects the reaction rate and therefore needs to be accounted for.

Very few studies have been conducted on this topic in the last decade and a half. The first prominent research paper dealing with the thermodynamic limitation responsible for the incomplete spending of organic acids at high pressure conditions was published by Chatelain et al. in 1976. After this, Fredd and Fogler (1998) and Buijse et al. (2004) developed distinct models to determine the reaction kinetics of organic acids with carbonates. The algorithm or workflows of these models are explained in detail in the following section of this chapter.

Chatelain et al. Model

Chatelain, Silberberg, and Schechter (1976) presented a correlation which accounts for the incomplete dissociation of organic acids at different acid concentration and temperature conditions. As per this study, the reaction of calcium carbonate with organic acid is considered to be a result of series of ionic reactions. These ionic reactions describing the complete organic acid/calcite interaction are given in eq. 2.1, 2.1, and 2.3.

$$2H^{+}_{(aq)} + CaCO_{3_{(s)}} \leftrightarrow Ca^{2+}_{(aq)} + H_2O_{(aq)} + CO_{2_{(aq)}} \quad 2.1$$

$$HA \leftrightarrow H^{+} + A^{-} \quad 2.2$$

$$Ca^{2+} + A^{-} \leftrightarrow CaA^{+} \quad 2.3$$

The equilibrium constants (k) for these equations in terms of their ionic activity coefficients (γ) and concentration are given as follows (Callen 1985):

$$k_1 = \frac{\gamma^3_{Ca^{2+}A^{-}} * \gamma_{CO_2}}{\gamma^4_{H^{+}A^{-}}} * \frac{[Ca^{2+}] * [CO_2]}{[H^{+}]^2} \quad 2.4$$

$$k_2 = \frac{\gamma^2_{H^{+}A^{-}}}{\gamma_{HA}} * \frac{[H^{+}] * [A^{-}]}{[HA]} \quad 2.5$$

$$k_3 = \frac{\gamma^2_{CaA^{+}A^{-}}}{\gamma^3_{Ca^{2+}A^{-}}} * \frac{[CaA^{+}]}{[Ca^{2+}][A^{-}]} \quad 2.6$$

Empirical constants based on the thermodynamic data of different organic acids can be used to determine the equilibrium constants. The ionic activity coefficients are known to be function of the interfacial concentration and therefore can be estimated if the concentration values are known. So, effectively we have a system of 3 equations with six unknown concentrations. This system cannot be mathematically solved unless additional data or information is added. The material balance equations listed from eq. 2.7 - 2.10 can simplify our study.

$$[CO_2] = \frac{1}{2}X\beta \quad (2.7)$$

$$[Ca^{2+}] + [CaA^{+}] = \frac{1}{2}X\beta \quad (2.8)$$

$$[A^{-}] + [CaA^{+}] = X\beta \quad (2.9)$$

$$[HA] = \beta(N - X) \quad (2.10)$$

Where X represents the number of moles of acid that reacts with 1000 gm of water in the original acid solution, N is the initial acid molality and β is given as:

$$\beta = \frac{1000}{1000 + 9X}$$

The only unknown in the four mass transfer equations (eq. 2.7 – 2.10) is X, so by combining these equations with the equilibrium equations (2.4 – 2.6), we will end up having a system of 7 equations and 7 unknowns. This system can then be reduced into the following two algebraic equations (eq. 2.11 and 2.12) having X and [Ca^{2+}] as unknowns.

$$K_3\left(\frac{\gamma_{HA} * \gamma^{3/2}_{Ca^{2+}A^{-}}}{\gamma^{2}_{CaA^{+}A^{-}} * \gamma^{1/2}_{CO_2}}\right) = \frac{\left(\frac{1}{2}X\beta - [Ca^{2+}]\right) * \left(\frac{1}{2}X\beta\right)^{1/2}}{K_1{}^{1/2} * K_2 * (N - X) * \beta * [Ca^{2+}]^{1/2}} \quad (2.11)$$

$$\left(\frac{\gamma_{HA}}{\gamma^{3/2}_{Ca^{2+}A^{-}} * \gamma^{1/2}_{CO_2}}\right) * \frac{K_1{}^{\frac{1}{2}} * K_2 * (N - X) * \beta}{\left(\frac{1}{2}X\beta\right)^{\frac{1}{2}} * [Ca^{2+}]^{\frac{1}{2}}} - [Ca^{2+}] = \frac{1}{2}X\beta \quad (2.12)$$

Simultaneously solving eq. 2.11 and 2.12 will result in determination of both $[Ca^{2+}]$ and the spent acid fraction, X. In addition, the correlations can also be used to establish the effect of temperature and initial acid concentration on the acid spending rate as all the value of equilibrium constants and ionic activity coefficients are dependent on these two parameters.

A major shortcoming of this approach is that it only focusses on estimating the spent acid fraction and does not consider the influence of either mass transfer or surface reaction parameters on the reaction kinetics.

Fredd and Fogler Model

A new approach involving a detailed analysis of the effect of mass transport and reversible reactions on the rock dissolution rate was suggested by Fredd and Fogler (1998). This study gives a comprehensive description of the kinetics of all the interfacial reactions that occurs between carbonate and acetic acid system. Impact or effect of each of the reversible reaction as well as the mass transfer parameters, on the overall reaction kinetics is accounted for in this model.

As described in the introduction, the overall reaction between an organic acid solution and a reactive rock can be categorized into three steps, which are the transport of reactants from the bulk solution to the rock surface, the surface reaction between the rock minerals and the reactants, and the transport of the generated products away from the interface. For a weak organic acid like acetic acid, rate limiting step is the surface reaction process and therefore it is important to analyze this step very carefully.

The reaction between acetic acid and calcium carbonate system accounts for various the interfacial reactions, which are listed in Table 2.1.

Equilibrium Reactions	
$HAc \leftrightarrow Ac^- + H^+$	log K = - 4.76
$CaAc^+ \leftrightarrow Ca^{2+} + Ac^-$	log K = - 0.77
$CaCO_3 \leftrightarrow Ca^{2+} + {CO_3}^{2-}$	log K = - 8.34
$CaHCO_3{}^+ \leftrightarrow Ca^{2+} + HCO_3{}^-$	log K = - 1.02
$CaOH^+ \leftrightarrow Ca^{2+} + OH^-$	log K = - 1.40
$CaCO_3{}^0 \leftrightarrow Ca^{2+} + {CO_3}^{2-}$	log K = + 3.26
$H_2O \leftrightarrow H^+ + OH^-$	log K = - 14.00
$H_2O + CO_2 \leftrightarrow HCO_3{}^- + H^+$	log K = - 6.37
$H_2CO_3{}^0 \leftrightarrow HCO_3{}^- + H^+$	log K = - 6.37
$HCO_3{}^- \leftrightarrow {CO_3}^{2-} + H^+$	log K = - 10.33
$NaAc \leftrightarrow Na^+ + Ac^-$	log K = - 1.06
$NaCO_3{}^- \leftrightarrow Na^+ + {CO_3}^{2-}$	log K = + 1.27
$Na_2CO_3{}^0 \leftrightarrow 2\,Na^+ + {CO_3}^{2-}$	log K = - 0.67
$NaHCO_3{}^0 \leftrightarrow Na^+ + HCO_3{}^-$	log K = + 0.25

Table 2.1: Equilibrium reactions for acetic acid/calcium carbonate system

The equilibrium constants for all these reactions at room temperature (25°C) were obtained from Truesdell and Jones (1974), Davies (1962) and Harned and Owen (1958). The above system of 14 equations contains 19 unknowns. The last four reactions including sodium species does not contribute to the reaction kinetics in acidic medium and therefore can be dropped out of the analysis. It should also be noted that the

formation of neutral specie $CaAc_2$ is not considered because the work of Nancollas (1956) showed that its concentration is negligible in presence of Ca^{2+} and $CaAc^{+}$.

A generalized form of all the surface reactions listed in Table 2.1 can be demonstrated by eq. 2.13.

$$Reactants + CaCO_3 \leftrightarrow Products \tag{2.13}$$

The reactants term includes both H^{+} as well as the undissociated acid (HA). The reaction products comprises of the calcium and carbonate species. Determination of mass transfer parameters for all the interfacial species individually is very difficult and can be simplified by grouping them together (Vitagliano, and Lyons 1956).

$$(H) = (H^{+}) + (HA) \tag{2.14}$$

$$(M) = (Ca^{2+}) + (CaAc^{+}) + (CaHCO_3{}^{-}) + (CaOH^{+}) \tag{2.15}$$

$$(CO) = (HCO_3{}^{-}) + \left(CO_3{}^{2-}\right) + (CO_2) + (H_2CO_3) \tag{2.16}$$

These interfacial grouped concentrations can be calculated using the dissolution rate equation of a rotating disk apparatus (RDA), which is explained in detail in the chapter 3. The addition of the grouped concentration equations into our system will not increase the number of unknowns and therefore we will end up having 17 equations with 19 variables.

$$(A) = (Ac^{-}) + (HAc) + (NaAc) \qquad 2.17$$

$$(N) = (Na^{+}) + (NaAc) + (NaCO_3{}^{-}) \qquad 2.18$$

Two independent correlations based on the overall charge neutrality and sodium species balance are represented in eq. 2.17 and 2.18. The value of (A) is determined such that the cumulative charge of the interfacial species is neutralized and (N) is assumed to be constant throughout the bulk fluid and the boundary layer. These two equations complete our system of 19 equations and 19 variables, which are solved iteratively to evaluate all the interfacial species concentration. The equilibrium constant values differ as per the temperature and initial acid concentration and therefore needs to be corrected. Extended form of Debye-Hückel equation (Eq. 2.19, Robinson and Stokes 1955) yields activity coefficient value which is used to correct the equilibrium constant.

$$\log \gamma = \frac{-Az^2\sqrt{I}}{1+Ba\sqrt{I}} + bI \qquad 2.19$$

Where A and B are solvent based constants, z corresponds to the ionic charge, I is the ionic strength, parameter a represents the hydrated ion size and parameter b allows for the decrease in solvent concentration in concentrated solutions. The values of all the constants are listed in Table 2.2 and Table 2.3. These results are used to determine the important kinetic parameters like the effective reaction rate constant (k_r), the conditional equilibrium constant (k_c), and the effective equilibrium constant (k_{eff}).

Temperature (°F)	Parameter A	Parameter B
80	0.5125	0.3294
150	0.5558	0.3384
200	0.6316	0.3466

Table 2.2: Values for A & B constants for water (Dean 1972)

Species	a parameter	b parameter
H^+	9	0
Ac^-	4.5	0
Ca^{2+}	6	0.165
$CaAc^+$	4.4	0
CO_3^{2-}	4.5	0
HCO_3^-	4	0
$CaHCO_3^+$	4.4	0
OH^-	3.5	0
$CaOH^+$	4.4	0

Table 2.3: Values for a & b parameters for each ionic species (Truesdell and Jones 1974)

The generalized form (Eq. 2.13) of the overall reactions can be modified in terms of the grouped species concentration (Eq. 2.19) and its corresponding conditional equilibrium constant is defined as follows:

$$[H] + CaCO_3 \leftrightarrow [M] + [CO] \quad 2.19$$

$$K_c = \frac{[M]*[CO]}{[H]} \quad 2.20$$

Fredd and Fogler (1998) found that the total interfacial concentration of carbonate species does not depend on the disk rotational speed and therefore can be consider as constant. This finding resulted in defining another parameter called as effective equilibrium constant which is nothing but a ratio of conditional equilibrium constant to the concentration of the carbonate species. Mathematically, it is given as $K_{eff} = \frac{K_c}{[CO]} = \frac{[M]}{[H]}$

At steady state condition, all the three steps of mass transfer of reactants, surface reaction rate, and mass transfer of the products are equal. Equating these process rates with each other yields the following expression:

$$r_D = \kappa \left[(H)_b - \frac{(M)_b}{k_{eff}} \right] \quad 2.21$$

$$\kappa = \frac{1}{\left(\frac{\nu}{K_{m,r}} + \frac{1}{K_r} + \frac{1}{K_{m,p} K_{eff}} \right)} \quad 2.22$$

Where, κ is the overall reaction rate constant, ν is the stoichiometric ratio of reactants consumed to the products generated, $K_{m,r}$ is the mass transfer coefficients of reactants, , K_r represents the effective forward reaction rate constant, $K_{m,p}$ describes the mass transfer coefficient of products and the terms with within the small parenthesis with subscript b corresponds to the bulk concentration of those species.

The overall rate of dissolution described in eq. 2.21 can also be expressed in a linearized form analogous to y = mx + c, where m is the slope and c represents the y-intercept of the line. For our case, this correlation is developed between reciprocal of dissolution rate and reciprocal of the square root of the rotational speed and it represented in eq. 2.23.

$$\frac{1}{r_D} = \frac{\left[\frac{\nu}{K_{m,r}} + \frac{1}{K_{eff}K^{*}m,p}\right]}{\left[(H)_b - \frac{(M)_b}{K_{eff}}\right]} * \frac{1}{\omega^{1/2}} + \frac{1}{k_r\left[(H)_b - \frac{(M)_b}{K_{eff}}\right]} \qquad 2.23$$

Experimental results can be used to develop a between $1/r_D$ and $1/\omega^{1/2}$. The slope and intercept of this plot depicts the first and the second term on the right hand side of the eq. 2.23, respectively. Additionally, percentage contribution of each step process on the overall reaction kinetics can be estimating by evaluating individual terms in the denominator of eq. 2.22.

This model is very robust, comprehensive and requires a lot of input data. Most of the input parameters vary with change in acid concentration, rock composition, and

temperature and pressure conditions and therefore their estimation is not easy. Even small error in these parameters can result in large variation in the results and therefore, this model requires appropriate measurement of various rock and fluid properties at different conditions as well as sound knowledge about the aspects of surface chemistry and reaction kinetics.

Buijse et al. Model

Buijse, Boer, and Breukel (2004) suggested a simple and general approach for the acid/carbonate system which can be used for all kind of acidic solutions. As per them, the reaction mechanisms of strong and weak acids are not similar solely because of the difference in their acid dissociation constants. Their model is based on a strong acid (HCl) model but includes an additional parameter of acid dissociation constant which enables it to be used for weak acid solutions as well.

Generally, the acid dissociation reaction at equilibrium condition and its corresponding dissociation constant are described as follows:

$$HA \leftrightarrow H^+ + A^- \qquad 2.24$$

$$K_A = \frac{H^+ * A^-}{HA} \qquad 2.25$$

Strong acids dissociate completely and thus have a very high acid dissociation constant, whereas the weak acids are known to have incomplete dissociation yielding lower k_A values. Table 2.4 (Fredd and Fogler 1998) indicates the dissociation constants

and the strength of few commonly used stimulation acids. It can be observed that the organic acids are very weak compared to HCl.

Acid Type	Dissociation Constant, K_A (mol/L)	Acid Strength (for 1 mol/L)	
		pH	$[H^+]$ (mol/L)
HCl	>>1	0	1
Formic acid	1.80E-04	1.9	0.013
Acetic acid	1.74E-05	2.4	0.004

Table 2.4: Dissociation constants and strength of acids

For strong acids, the reaction rate equation is given as eq. 2.26, where k is the reaction rate constant, $[H]_s$ corresponds to the concentration of hydrogen ion at the reaction surface and n represents the reaction order.

$$R_{kin} = k.[H^+]_s^n \qquad 2.26$$

Eq. 2.26 governs the surface reaction process, but for the strong acids, the mass transfer process is limiting step and therefore a correlation describing the rate of mass transfer of both reactants and products needs to be developed. Eq. 2.27 explains the rate of diffusion process.

$$R_{MT} = K_{MT}\,([H^+]_b - [H^+]_s) \qquad 2.27$$

Where K_{MT} is the mass transfer coefficient and $[H^+]_b$ and $[H^+]_s$ corresponds the hydrogen ion concentration at bulk and interface, respectively. At steady state condition, the rate of surface reaction and the rate of diffusion is equal. Assuming that the reaction is a first order reaction (n = 1), we can represent the overall reaction rate as follows:

$$R = \frac{k* K_{MT}}{k+ K_{MT}} [H^+]_b \qquad 2.28$$

For a strong acid system, where the surface reaction is very rapid, the value of reaction rate constant is very high compared to the mass transfer coefficient ($k >>> K_{MT}$). Therefore, the overall reaction rate will be linearly dependent on the bulk concentration of H^+. Physically, it signifies that if we increase the acid concentration then the reaction rate will also increase proportionally. The same is not the case with weak organic acids as they do not dissociate completely and therefore the appropriate rate of mass transport is given by eq. 2.29.

$$R_{MT} = K_{MT} (C_b - C_s) \qquad 2.29$$

Where, the undissociated acid concentrations at the bulk and surface are given by C_b and C_s respectively. Both the mass transfer equations for strong and weak acids are similar with the only difference being that in eq. 2.27, the H^+ exists in dissociated state in the bulk and gets diffused to the reaction surface, whereas in eq. 2.29, the undissociated acid dissociates after being diffused to the surface. A combined model should incorporate both these phenomenon within itself and only then it can be used for both strong as well as weak acid system. To achieve this, the sum of the concentrations of H^+ and undissociated acid HA is taken together to define total acid concentration (C). An important relationship that correlates the total acid concentration at the reaction surface (C_s) with the acid dissociation constant (K_A) was developed in this study and is represented in eq. 2.30.

$$C_s = [H^+]_s + [HA]_s = [H^+]_s + \frac{[H^+]_s * C_o}{[H^+]_s + K_A} \quad 2.30$$

The mass transfer rate for an acid system can be determined by substituting the value of C_s in eq. 2.29. Again at steady state condition and for a first order reaction between the rock and the acid system, the overall reaction rate can be written as:

$$R \,.\left(1 + \frac{R}{k.K_A}\right) = \frac{k.K_{MT}}{k + K_{MT}} \,.C_o \quad 2.31$$

Comparing eq. 2.31 with eq. 2.28 signifies that the term $\left(1 + \frac{R}{k.K_A}\right)$ accounts for the lower spending of the weak acids compared to strong acids.

In order to incorporate the effect of reversible reactions on the reaction, a new parameter X is defined. The value of parameter X is related to the calcium carbonate solubility product as well as the equilibrium constants of the carbonic acid reactions. The final form of the overall rate of reaction which accounts for the reversible reaction and can be applied to both strong and weak acids is shown in eq. 2.32.

$$R_{kin} = k.\left([H^+]_s^n - X^n.\frac{(C_0 - C_s)^{2n}}{[H^+]_s^n}\right) \quad 2.32$$

This model is developed on the basis of the reaction of either dissociated H^+ or the undissociated acid concentrations and does not consider the effect of all the intermediate species that are generated while the acid and rock mineral interacts. It also considers that the reaction rate of strong and weak acids differ solely because of the difference between their acid dissociation constants. Moreover, the reaction rate constant

(k) and the reaction order (n) are not believed to affect the reaction rate and were considered same for all types of acid systems.

All the three models explained in this chapter were analyzed and experimental analysis was carried out to establish the accuracy and effectiveness of these models to the lab scale results.

CHAPTER III

MATERIALS AND EQUIPMENT

The porosity, mineralogy and composition of the reservoir rock as well as the rheological properties of the acid systems can significantly affect the reaction rate of an acid treatment. So, it is important to measure these parameters accurately at different conditions. Determination of all the aforementioned properties can be achieved by conducting a number of experimental studies described as following section.

Rock Properties

Marble (calcite) disks of known diameter and thickness (1.5” diameter and 0.6” thickness) were used for the following analysis.

Porosity

The conventional method of porosity determination involves saturating the cores with a fluid of known density and measuring the difference in weight of the saturated and dry cores. The ratio of weight difference to fluid density gives the pore volume of the rock, which is then divided by the bulk volume to estimate the porosity. This approach cannot work for a marble disk as it is known to have very low porosity and therefore, its saturation will not result in significant increment in weight. In order to accurately measure the marble disk porosity, Helium Porositimeter (Fig. 3.1) was used.

Figure 3.1: Helium Porositimeter

The governing principle of this device is Boyle's law, according to which, for a fixed mass of gas and at isothermal condition, the product of absolute pressure and volume always remain constant. As shown in the diagram, the porositimeter consists of a compact chamber, which is firstly filled with metallic disks of known thickness and pressurized by the injection of Helium gas. The corresponding pressure reading is averaged out and noted down. Subsequently, some metallic disks are replaced by a marble disk of similar dimension and the process is repeated. The pressure variation obtained between the two cases is equated to calculate the incremental pore volume of the marble. The ratio of pore volume to the bulk volume represents the porosity of the marble disk.

Composition

The mineralogy of the rock surface reacting with the acid can be estimated by performing an X-ray Fluorescence (XRF) analysis. In this technique, the disk surface is bombarded with high energy X-rays or gamma rays and the emission of characteristic secondary wavelets are analyzed to determine the composition of the solid rock surface. The schematic of a XRF is shown in Fig. 3.2. For this study, a cut-off value of 97% calcium oxide (CaO) was set to make sure that only high purity cores are chosen for the rotating disk apparatus experiments. Having a composition screen reduces the presence of impurities at the rock surface and therefore negates their impact on the reaction kinetics.

Figure 3.2: X-Ray Fluorescence

Fluid Properties

Rheological properties of acetic acid solutions (0.5, 1.0, 1.5, and 2.0 molar concentrations) at different temperature conditions were carried out by the following methods:

Density

Density of a substance is defined as the ratio of its mass to its volume. The density of a fluid varies with change in temperature and therefore it is important to measure it accurately at all the different temperature conditions.

At room temperature, density measurements were done using a pycnometer. A pycnometer is a simple glass flask whose dry weight and volume are known. A sample fluid is then used to fill the pycnometer completely and the gas bubbles (if any present) are expelled out. The incremental weight gain is then measured, which corresponds to the weight of the known volume of the sample and hence the fluid's density is estimated.

At higher temperature conditions, instead of pycnometer, a high temperature high pressure densitimeter was used. This equipment can determine the density of the fluid sample injected at different temperature conditions ranging from 32-200°F. Fig. 3.3 shows both these devices.

Figure 3.3: Pycnometer and High Temperature Densitimeter

Viscosity

A fluid's resistance to flow is defined as its viscosity. Similar to density, fluid's viscosity also varies with temperature. Use of capillary viscometer is the simplest way to measure the viscosity of a Newtonian fluid. A capillary viscometer consists of three capillary tubes of different diameters. Small volume of sample (about 10 cm^3) is injected into the capillary and the entire system is then immersed in an oil bath. The temperature of the oil bath can be controlled and the once the stabilized temperature condition is reached, the sample is raised through the biggest capillary tube by using a vacuum pump. The fluid is then allowed to drop down as per the gravitational force and the time taken by it to move from point 1 to point 2 is recorded. This time is used to determine the kinematic viscosity of the sample.

Dynamic viscosity was measured by multiplying the kinematic viscosity of the fluid with its density at the given temperature.

Reaction Rate Analysis

The rock and acid solution were allowed to interact at different conditions and the effluent samples were analyzed to determine the rate of reaction. Two important equipment that were used for this estimation are described below.

Rotating Disk Apparatus

The overall reaction of a rock with an acid solution is a very complex process due to the influence of transport phenomenon along with the surface reaction. A simplistic model of fluid flow over a flat plate system was initially developed with a laminar boundary layer flow solution (Schlichting 1960). This approach had many disadvantages and shortcomings like necessity of a flow tunnel and a large volume of reacting acid, high edge and end-effects, two dimensional flow solutions (Litt, and Serad 1964).

A rotating disk apparatus can overcome all the aforementioned drawbacks (Boomer, McCune, and Fogler 1972). It is also shown that if the diameter of the reaction vessel is at least double the disk diameter, then the mass transport rate is independent of the vessel diameter (Gregory and Riddiford 1956). In order to maintain laminar flow at the rotating disk surface, the Reynolds number ($R_e = \omega R^2/\nu$) should not exceed 2.5 x 10^5 (Ellison and Cornet 1971). For the experimental study undertaken in this work, the Reynolds number corresponds to 3440 rpm at the highest temperature condition of 250°F, where the kinematic viscosity of acetic acid solution is lowest. Moreover, study conducted by Levich (1962), suggested that in order to maintain a negligible boundary layer thickness compared to the disk diameter, the Reynolds number should be

approximately 10. Rotational speed of 0.75 rpm at room temperature, where the kinematic viscosity will be the highest, corresponds to this condition. All the experiments were conducted at rotational speeds between 100-1500 rpm, which are well within the specified limits to have a laminar flow regime and no impact of boundary layer thickness.

The mass flux of solute from the bulk solution to the rotating disk surface, under laminar condition is given by following equation (Newman 1996):

$$J\ (\mathrm{gmol}/cm^2.\sec) = \left[\frac{0.62048 * {S_c}^{-2/3} * \sqrt{\nu\omega}}{0.2980 * {S_c}^{-1/3} + 0.1451 * {S_c}^{-2/3}}\right](C_b - C_i) \qquad 3.1$$

Where, Sc (Schmidt number) is defined as the ratio of kinematic viscosity (ν) to the diffusion coefficient (D) of the fluid solution, ω represents the rotational speed of the disk, Cb and Ci are the bulk and interfacial concentrations respectively.

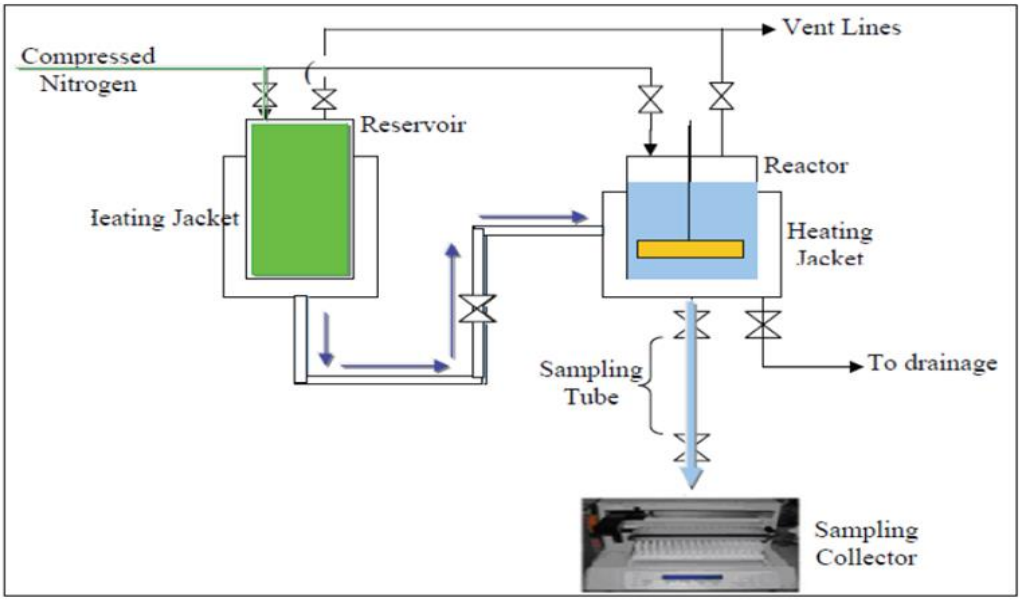

Figure 3.4: Rotating Disk Apparatus (Rabie et al. 2014)

Fig. 3.4 depicts the schematic of an RDA, which mainly comprises of two cylindrical chambers viz. primary reactor cell and pre-charge reservoir cell. Both these cells are fabricated using Hastelloy B alloy to prevent it from acid corrosion and are covered with heating jackets. Stimulation fluid is introduced into the reservoir cell and its temperature is raised to the desired experimental temperature. The reactor chamber comprises of a core holder connected to a long magnetic shaft, which enables the rotation of the disk. A rock sample is attached to the core holder using heat shrinkable Teflon tubing and placed inside is the reactor chamber. Once the experimental pressure and temperature conditions are reached, the acid is injected from the reservoir to the reactor to start the reaction between acid and rock. Simultaneously, the core is allowed to rotate at a set RPM so as to generate radial flow profile representative of the actual acid injection system in the field. The effluent fluid samples are collected periodically, which results in reduction of reactor pressure. This pressure reduction can cause generated CO_2 to liberate as free gas bubbles that can affect the acid reaction with carbonate (Plummer, Wigley, and Parkhurst 1978) and also disrupt the laminar flow on the rock surface (Taylor, and Nasr-El-Din 2009). In order to prevent these problems, special consideration was given to keep the reactor pressure above 1000 psi to keep the CO_2 in solution.

Inductively Coupled Plasma

The RDA effluent samples, containing the dissolved rock minerals, were analyzed for their composition using Perkin Elmer 7000 DV Inductively Coupled Plasma – Optical Emission Spectroscopy (ICP/OES). ICP, as shown in Fig. 3.5, works on the principle of spontaneous emission of photons from atoms or ions that get excited in a radiofrequency induced argon plasma (Hou, and Jones 2008). The energized particles are unstable and tend to stabilize by achieving a lower energy state. The release in energy in the form of photon emission of each element follows a unique wavelength signature or trend. The number of photons emitted for each wavelength signature is used to determine the elemental composition of the fluid sample.

Figure 3.5: Inductively Coupled Plasma

CHAPTER IV

EXPERIMENTAL RESULTS AND ANALYSIS

Rotating disk experiments were carried out using acetic acid solutions on calcite marble disks at different temperatures (80, 150, 200, and 250°F), acid concentrations (0.5, 1.0, 1.5, and 2.0 molar), and disk rotational speeds (100 - 1700 RPM) using a rotating disk apparatus. Preparation of acid solutions were done by using deionized water with resistivity higher than 18 MΩ/cm at room temperature and appropriate corrosion inhibitor (approximately 0.1 vol. %). As stated in the chapter II, various properties of cores as well as the acid solutions were analyzed before being used in the RDA experiments. The measurements of these properties are important for the estimation of different kinetic and mass transfer parameters.

Porosity can greatly affect the surface area available for the acid to etch through and interact with the rock minerals. Helium porositimeter was used to measure the porosity of all the marble disks. Table 4.1 includes the results of two sample disks from the same marble slab. An average porosity value of 1.5% was estimated for the tested marble slab.

Apart from porosity, the mineral composition of the rock surface was also measured using X-Ray fluorescence techniques. A cut-off limit of 97% calcium oxide (CaO) was assigned and only the core samples having higher values were used for the reaction rate analysis. Table 4.2 indicates the compositional analysis results of some of the tested core samples. It can be observed that disk 50 had high amount of impurities in

the form of magnesium and sodium oxides which will give lower calcium dissolution rates compared to other core samples and therefore it was discarded.

CORE 10		
V1	10	cc
V2	25	cc
V_t	35	cc
Pa	13.92	
P1	70.03	
P12	98.76	
P2	92.63	
P_He	115.33	
Pore Volume		
	8.073427	
	7.210011	
	6.835809	
Average	**7.373082**	
Diameter	3.7846	
Thickness	1.60274	
V_b	18.02988	
Φ	**1.2%**	

CORE 11		
V1	10	cc
V2	25	cc
V_t	35	cc
Pa	13.92	
P1	75.4	
P12	97.09	
P2	90.65	
P_He	115.33	
Pore Volume		
	6.494795	
	8.041183	
	7.675845	
Average	**7.403941**	
Diameter	3.7846	
Thickness	1.6002	
V_b	18.00131	
Φ	**1.0%**	

Table 4.1: Porosity measurement of marble disks

Sample 46	
Formula	Concentration
CaO	99
Al2O3	0.347
SiO2	0.237
K2O	0.125
Cl	0.0786
Fe2O3	0.062
SrO	0.0396
SnO2	0.0293

Sample 47	
Formula	Concentration
CaO	98.5
SiO2	0.451
Al2O3	0.409
K2O	0.269
Cl	0.234
Fe2O3	0.0653
SrO	0.0529
SnO2	0.0297

Sample 48	
Formula	Concentration
CaO	98.7
SiO2	0.504
Al2O3	0.398
K2O	0.175
Fe2O3	0.0698
Cl	0.067
SrO	0.0479
SnO2	0.0296

Sample 49	
Formula	Concentration
CaO	98.6
SiO2	0.54
Al2O3	0.325
K2O	0.184
Cl	0.179
Fe2O3	0.0785
SrO	0.045
SnO2	0.0289

Sample 50	
Formula	Concentration
CaO	83.7
MgO	10.2
Na2O	4.06
Cl	0.743
SiO2	0.559
Fe2O3	0.294
P2O5	0.208
K2O	0.154
SrO	0.048
SnO2	0.0264
CdO	0.0134

Sample 51	
Formula	Concentration
CaO	98
MgO	0.775
Cl	0.161
SiO2	0.264
Al2O3	0.458
Fe2O3	0.0691
K2O	0.133
SrO	0.0485
SnO2	0.0282

Sample 52	
Formula	Concentration
CaO	98.5
Cl	0.394
SiO2	0.499
Al2O3	0.322
Fe2O3	0.0505
K2O	0.181
SrO	0.0342
SnO2	0.029

Sample 53	
Formula	Concentration
CaO	99.5
Cl	0.12
Fe2O3	0.0664
K2O	0.194
SrO	0.047
SnO2	0.0306

Sample 54	
Formula	Concentration
CaO	97.8
MgO	0.745
Cl	0.0611
SiO2	0.615
Fe2O3	0.0497
K2O	0.142
SrO	0.0521
SnO2	0.0286

Table 4.2: Compositional analysis of the marble disks

Densities of different acid solutions (0.5, 1.0, 1.5, and 2.0 M) at various experimental temperature conditions were measured using pycnometer and high temperature high pressure densitimeter. Table 4.3 and 4.4 enlists the calculated density values at room temperature and higher temperature conditions, respectively.

Density Measurement at Room Temperature				
Volume of Pycnometer				25 ml
Acid Conc. (mol/L)	Dry weight of Pycnometer (gm)	Weight of Pycnometer fully filled with acid (gm)	Weight of acid (gm)	Density of acid (gm/cc)
0.5	21.82	46.84	25.02	1.0008
1.0		46.91	25.09	1.0036
1.5		47.04	25.22	1.0088
2.0		47.12	25.3	1.012

Table 4.3: Density measurement at room temperature

High Temperature Density Mesurement						
Acid Conc. (mol/L)	100°F		150°F		200°F	
	Density	Avg. Density	Density	Avg. Density	Density	Avg. Density
0.50	0.9961	**0.9961**	0.9729	**0.9728**	0.8876	**0.8873**
	0.9961		0.9728		0.8873	
	0.9961		0.9726		0.8871	
1.00	0.9993	**0.9993**	0.9825	**0.9819**	0.9248	**0.9206**
	0.9993		0.9814		0.9171	
	0.9993		0.9819		0.9200	
1.50	1.0033	**1.0033**	0.9865	**0.9856**	0.9382	**0.9320**
	1.0033		0.9852		0.9249	
	1.0033		0.9852		0.9330	
2.00	1.0065	**1.0065**	0.9897	**0.9889**	0.9402	**0.9353**
	1.0065		0.9885		0.9331	
	1.0065		0.9885		0.9326	

Table 4.4: Density measurement at high temperatures

The kinematic viscosity of different acetic acid solutions were measured over a temperature range of 75-200°F using a capillary viscometer and are given in Table 4.5. Extrapolation of the calculated data points was done in order to estimate the viscosity values at temperature conditions higher than 200°F. Fig. 4.1 represents the variation trend shown by 0.5 M acetic acid solution with change in temperature.

VISCOSITY VARIATION WITH TEMPERATURE

At Room Temperature

Acid Conc.	Efflux times (Sec)				Viscometer	Kinematic Viscosity	Density	Dynamic Viscosity	Dynamic Viscosity
(mol/L)	T1	T2	T3	Avg. T	Constant	(Centi-Stokes)	(gm/cc)	(Centi-Poise)	(Pascal - Sec)
0.5	307	309	310	308.67	0.003	0.9260	1.0008	0.9267	0.000927
1	322	329	330	327		0.9810	1.0036	0.9845	0.000985
1.5	347	353	355	351.67		1.0550	1.0088	1.0643	0.001064
2	359	366	361	362		1.0860	1.0120	1.0990	0.001099

At 100°F (37.77°C)

Acid Conc.	Efflux times (Sec)				Viscometer	Kinematic Viscosity	Density	Dynamic Viscosity	Dynamic Viscosity
(mol/L)	T1	T2	T3	Avg. T	Constant	(Centi-Stokes)	(gm/cc)	(Centi-Poise)	(Pascal - Sec)
0.5	227	226	227	226.67	0.003	0.6800	0.9961	0.6773	0.000677
1	241	244	239	241.33		0.7240	0.9993	0.7235	0.000723
1.5	247	250	250	249		0.7470	1.0033	0.7495	0.000749
2	258	261	260	259.67		0.7790	1.0065	0.7841	0.000784

At 150°F (65.56°C)

Acid Conc.	Efflux times (Sec)				Viscometer	Kinematic Viscosity	Density	Dynamic Viscosity	Dynamic Viscosity
(mol/L)	T1	T2	T3	Avg. T	Constant	(Centi-Stokes)	(gm/cc)	(Centi-Poise)	(Pascal - Sec)
0.5	138	146	145	143	0.003	0.4290	0.9728	0.4173	0.000417
1	152	150	150	150.67		0.4520	0.9819	0.4438	0.000444
1.5	157	157	158	157.33		0.4720	0.9856	0.4652	0.000465
2	162	162	162	162		0.4860	0.9889	0.4806	0.000481

At 200°F (93.33°C)

Acid Conc.	Efflux times (Sec)				Viscometer	Kinematic Viscosity	Density	Dynamic Viscosity	Dynamic Viscosity
(mol/L)	T1	T2	T3	Avg. T	Constant	(Centi-Stokes)	(gm/cc)	(Centi-Poise)	(Pascal - Sec)
0.5	106	105	106	105.67	0.003	0.3170	0.8873	0.2813	0.000281
1	110	108	108	108.67		0.3260	0.9206	0.3001	0.000300
1.5	116	118	116	116.67		0.3500	0.9320	0.3262	0.000326
2	118	119	119	118.67		0.3560	0.9353	0.3330	0.000333

Table 4.5: Viscosity values of different acid solutions at various temperatures

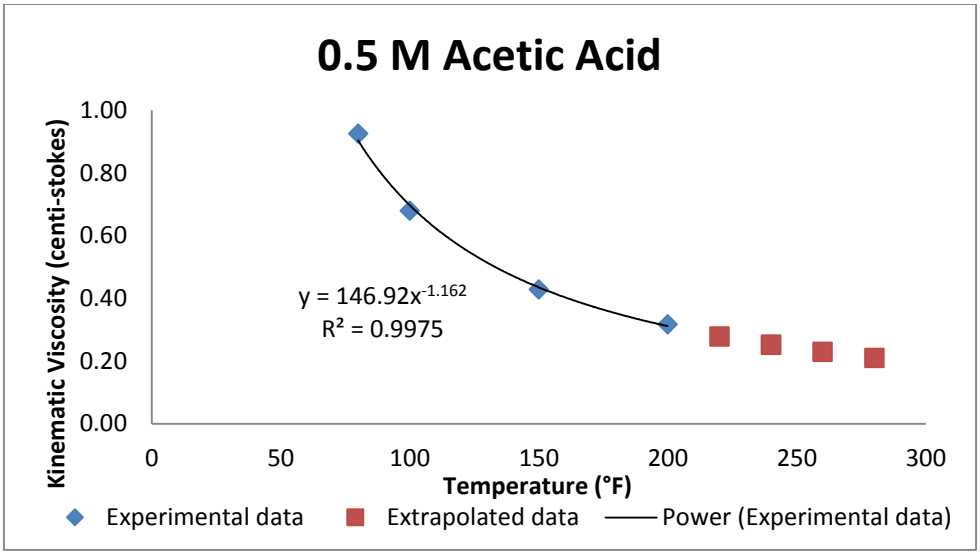

Figure 4.1: Kinematic viscosity calculations at higher temperature conditions

The diffusion coefficient values of acetic acid solutions at 25°C (77°F) were estimated by referring to Fig. 4.2 (Williams, Gidley, and Schechter, 1979).

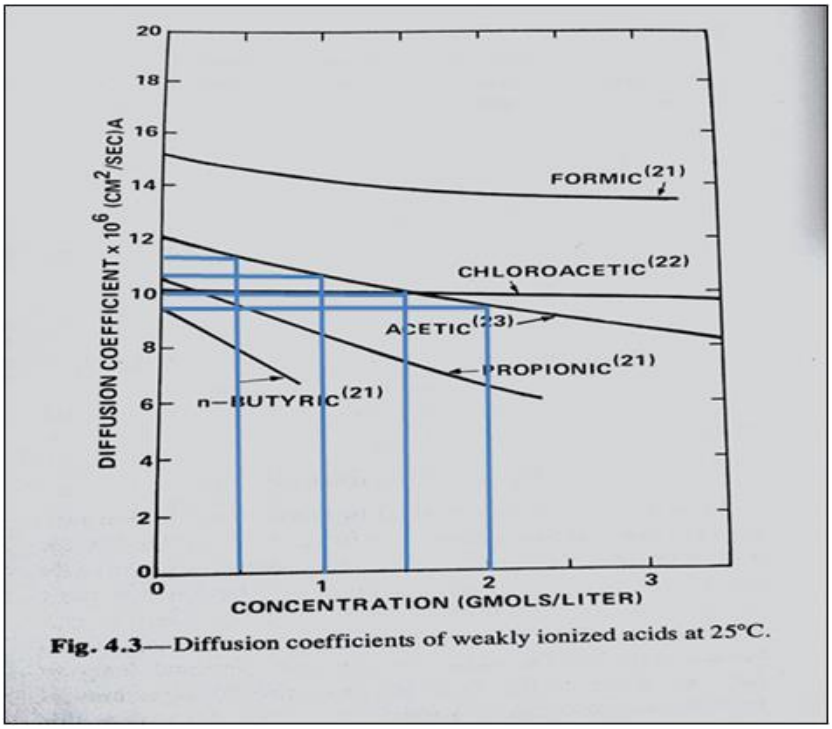

Figure 4.2: Diffusion coefficients at 25°C

At higher temperature conditions, the diffusion coefficients are required to be corrected. This correction can be achieved by either using the Arrhenius equation (Levich 1962) or the Stokes-Einstein equation. Generally, Arrhenius equation provides accurate diffusivity for solid particles whereas Stokes-Einstein is used for the liquid diffusivity estimation. In this study, the temperature dependence of diffusion coefficient was calculated using both these methods as our system comprises of both liquid acid ions as well as solid mineral ions.

Arrhenius equation of diffusivity is given by Eq. 4.1, where D represents the diffusion coefficient (cm^2/s), D_0 is the maximum diffusion coefficient (at infinite temperature, cm^2/s), E_a corresponds to the activation energy for diffusion (J/mol), T is the temperature (K), and R signifies the gas constant (J/K-mol).

$$D = D_0 e^{\frac{-E_a}{RT}} \qquad 4.1$$

The calculated diffusion coefficient values using Arrhenius equations are shown in Table 4.6.

Temperature (°F)	**Temperature (K)**	**D (cm^2/sec)**			
		0.5 M	**1 M**	**1.5 M**	**2 M**
77	**298.15**	1.1250E-05	1.0500E-05	1.0000E-05	9.5000E-06
150	**338.7056**	2.4345E-05	2.2722E-05	2.1640E-05	2.0558E-05
200	**366.4833**	3.7429E-05	3.4934E-05	3.3270E-05	3.1607E-05
250	**394.261**	5.4162E-05	5.0551E-05	4.8144E-05	4.5737E-05

Table 4.6: Corrected Diffusion coefficients - Arrhenius equation

Eq. 4.2 represents the Stokes-Einstein equation for the diffusivity of liquid particles. D and T denote the diffusion coefficient (cm^2/sec) and absolute temperature (K), and μ represents the dynamic viscosity of the solvent (Pa-sec). The corrected diffusion coefficient values by this approach are given in Table 4.7.

$$\frac{D_{T_1}}{D_{T_2}} = \frac{T_1}{T_2}\frac{\mu_{T_2}}{\mu_{T_1}} \qquad 4.2$$

Temperature (°F)	**Temperature (K)**	**D (cm2/sec)**			
		0.5 M	**1 M**	**1.5 M**	**2 M**
77	**298.15**	1.1250E-05	1.0500E-05	1.0000E-05	9.5000E-06
150	**338.7056**	2.8380E-05	2.6461E-05	2.5990E-05	2.4679E-05
200	**366.4833**	4.5562E-05	4.2340E-05	4.0104E-05	3.8544E-05

Table 4.7: Corrected Diffusion coefficients – Stokes-Einstein equation

It can be observed that both these approaches give very similar results and a comparison (Fig. 4.3) between the corrected diffusivity values calculated by both the methods yields negligible difference.

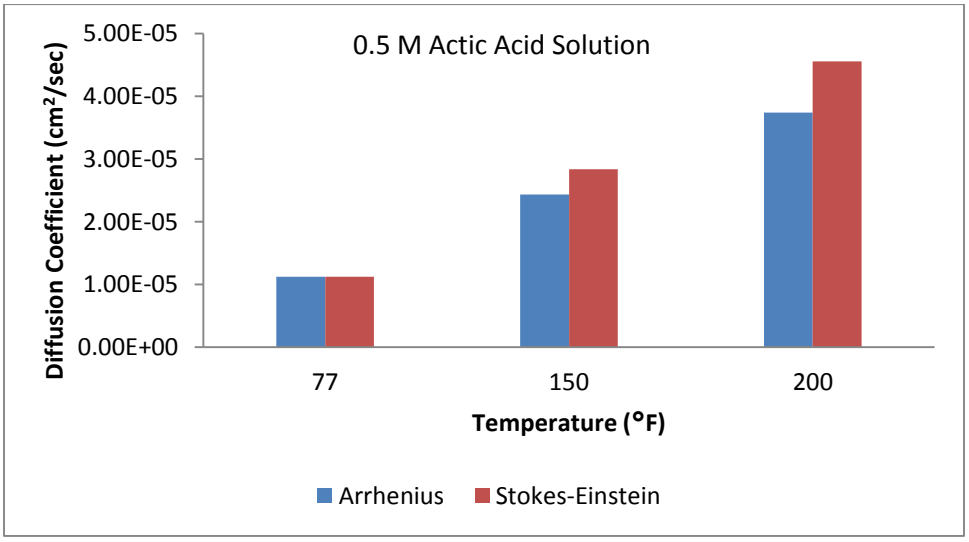

Figure 4.3: Corrected Diffusion Coefficients

The calcium dissolution rate is determined experimentally by using the plot between moles of calcium liberated versus time. The effluent samples collected periodically from the RDA experiments are diluted and analyzed in the ICP-OES for calcium concentration. The mass of calcium liberated is then corrected and the cumulative calcium concentration including the amount of calcium present in the reactor chamber is estimated. The slope of total moles of calcium liberated with respect to time gives the rate of calcium dissolution for the given disk surface area. At each temperature condition, this analysis is carried out for 4 different acid concentrations and 7 distinct rotational speeds. Results corresponding to 0.5 Molar acetic acid solutions at 150°F over a range of rotational speeds (100-1500 RPM) are shown in Fig. 4.4. All the other experimental results (28 experiments each for 2 other temperature conditions) are included in the appendix section of this work.

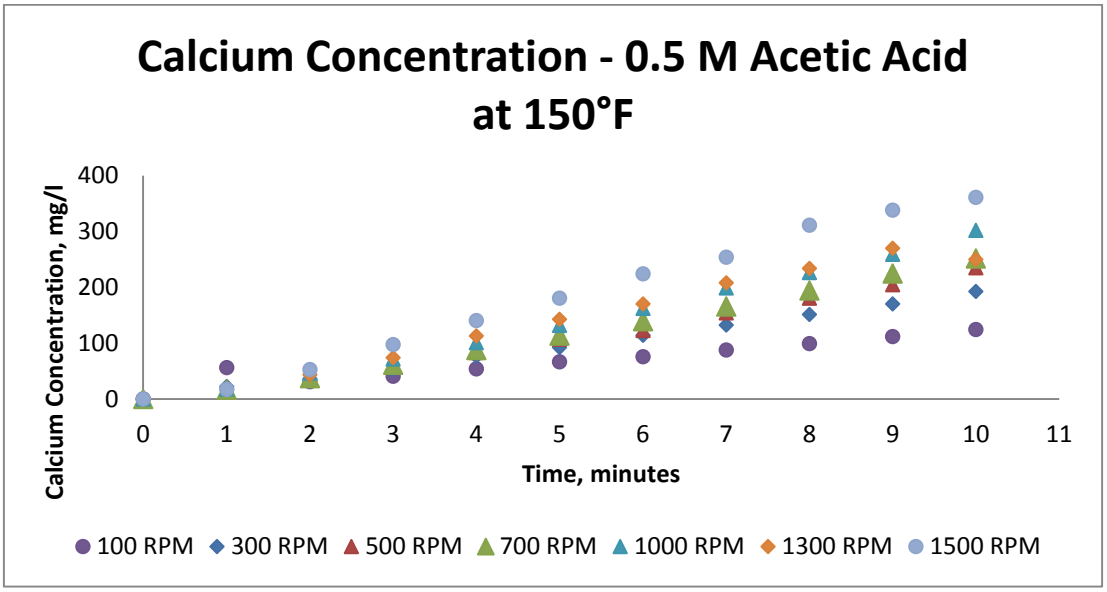

Figure 4.4: Calcium liberation rate

Apart from the reaction rate determination, another important inference that can be derived from these plots is the reaction regime. As described in the previous chapter, the calcium ion flux follows Eq. 3.1 and therefore if the dissolution rate increases linearly with the increment in square root of disk rotational speed (√ω), then it is said to follow a mass transfer limited regime. On the other hand, if the increase in √ω does not cause any effect the dissolution rate, then the process is believed to follow a surface reaction limited regime. It can be seen from Table 4.8 and Fig. 4.5, that the reaction of 0.5 M acetic acid solution with calcite at 150°F is mass transfer limited.

RPM	ω	ω^1/2	Dissolution rate
100	10.46667	**3.235223**	**4.17E-07**
300	31.4	**5.60357**	**6.80E-07**
500	52.33333	**7.234178**	**8.44E-07**
700	73.26667	**8.559595**	**9.03E-07**
1000	104.6667	**10.23067**	**1.09E-06**
1300	136.0667	**11.66476**	**1.14E-06**
1500	157	**12.52996**	**1.46E-06**

Table 4.8: Experimental dissolution rates

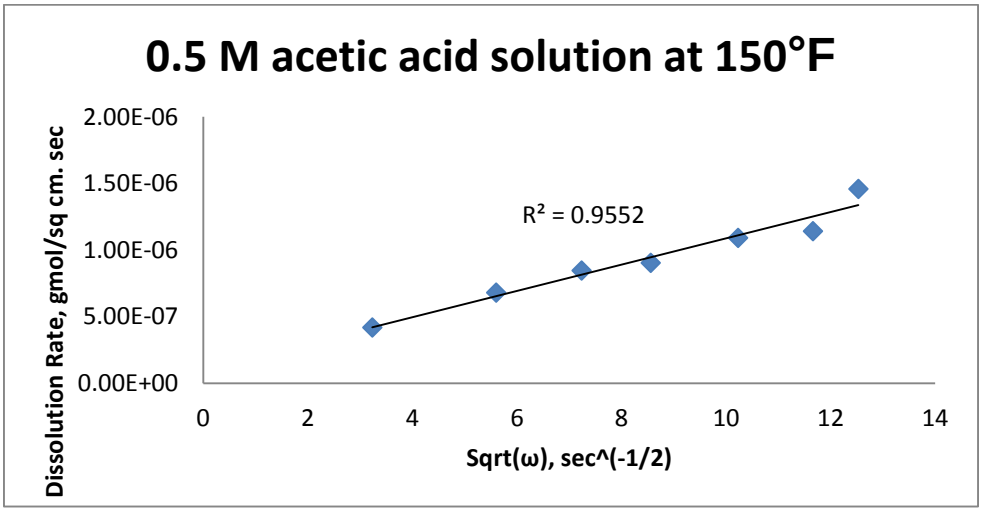

Figure 4.5: Reaction rate curve - 0.5 M acetic acid at 150°F

The experimentally determined reaction rates can be used to calculate the activation energy of the reaction. This can be done by first calculating the Schmidt number corresponding to the experimental reaction rate using Eq. 3.1 and then estimating the diffusion coefficient of the fluid. The slope of the plot of natural log of the diffusion coefficient versus the reciprocal of the absolute temperature yields the value of activation energy. The effect of reversible reaction on the overall reaction kinetics can be quantified by accurate estimation of the activation energy. An important assumption related to calculation of diffusion coefficient from the experimental reaction rate data is the negligible presence of the reactant concentration at the reaction surface. This assumption holds good for the strong acid systems as the acid dissociates and reacts completely with the rock minerals. Contrarily, due to the occurrence of reversible reactions, both reactants and products exist in equilibrium at the mineral-fluid interface.

Study conducted by Vitagliano and Lyons (1956) highlights the activation energy value for a purely diffusion limited reaction of undissociated acetic acid as 3.817 Kcal/mol. Table 4.9 includes the experimental data obtained for 0.5 M acetic acid solutions at three different temperature conditions, viz. room temperature (80°F), 150 and 200°F. Using these data points, the Schmidt number and diffusion coefficients were calculated as shown in Table 4.10. Fig. 4.6 was plotted to determine the calculated activation energy as 5.87 Kcal/mol. The difference between calculated and expected values represents the effect of reversible reactions and makes it imperative to consider the thermodynamic limitation associated with organic acids.

			Dissolution rate (gmole/cm^2-sec)		
RPM	**ω**	**ω^1/2**	**80°F**	**150°F**	**200°F**
100	10.46667	**3.235223**	**1.33E-07**	**4.17E-07**	**6.38E-07**
300	31.4	**5.60357**	**2.69E-07**	**6.80E-07**	**1.19E-06**
500	52.33333	**7.234178**	**2.24E-07**	**8.44E-07**	**1.72E-06**
700	73.26667	**8.559595**	**3.23E-07**	**9.03E-07**	**1.88E-06**
1000	104.6667	**10.23067**	**4.43E-07**	**1.09E-06**	**2.31E-06**
1300	136.0667	**11.66476**	**5.90E-07**	**1.14E-06**	**2.34E-06**
1500	157	**12.52996**	**5.22E-07**	**1.46E-06**	**2.56E-06**

Table 4.9: Dissolution rates of 0.5 M acetic acid at different temperatures

Temp (F)	Temp (K)	1/T	De (cm^2/sec)	ln (De)
80	299.8167	**0.003335**	**6.76029E-05**	**-9.60186**
150	338.7056	**0.002952**	**0.000159974**	**-8.7405**
200	366.4833	**0.002729**	**0.000427223**	**-7.75821**

Table 4.10: Calculated diffusion coefficients – Fredd and Fogler

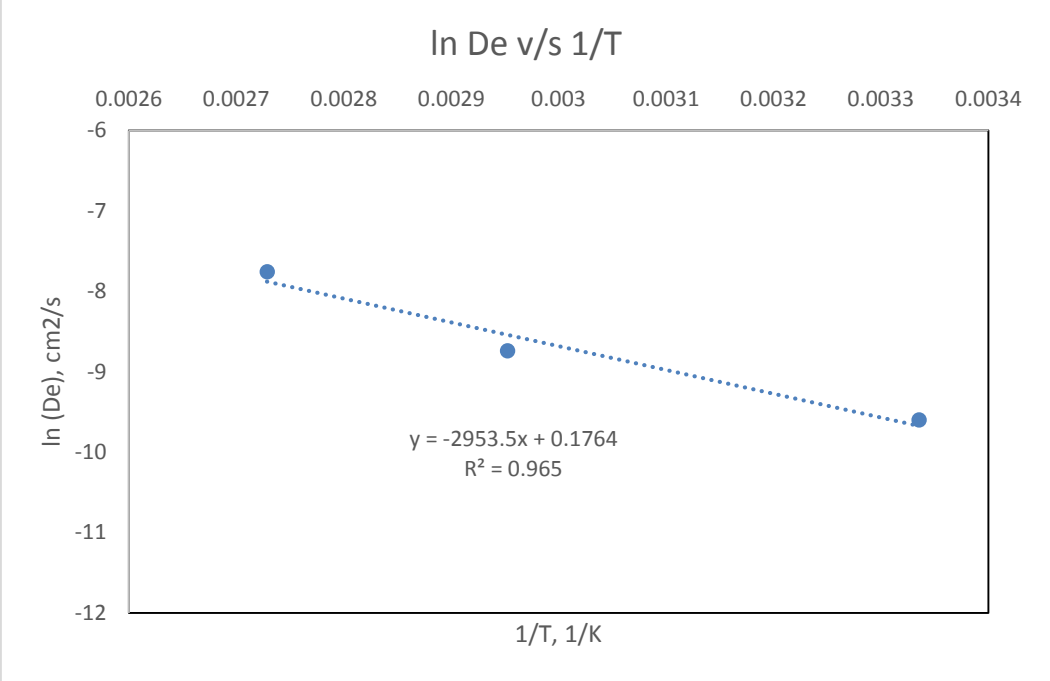

Figure 4.6: Estimation of activation energy

CHAPTER V

COMPARATIVE STUDY

The experimentally determined values of various parameters like reaction rates, diffusion coefficients and activation energies can be compared to the corresponding results obtained from different theoretical models. The coherence and accuracy of the calculated model results with the experimental results points towards the validity of these models and also highlights their effectiveness in estimating the different mass transfer and reaction kinetics parameters.

As mentioned in chapter II, the approach described by Chatelain et al. (1976) did not include the influence of either kinetic or mass transfer parameters and therefore was could not be used for a comparative analysis. The workflow or algorithm associated with Fredd and Fogler approach (1998) and Buijse's et al. method (2004) was developed as a part of this study and values of various parameters estimated by both these processes were compared to the experimentally obtained values.

As per the Fredd and Fogler approach, a system of 19 equations and 19 variables were solved iteratively at each experimental condition. The published data for reaction rates corresponding to 0.5 M and 1.0 M acetic acid solutions at room temperature is compared to the experimentally determined reaction rates in Table 5.1. These values are close to each other (Fig. 5.1 and 5.2) and the variation between them could be because of inaccuracy in viscosity or reaction rate measurement. Also the diffusion coefficients

estimations at higher temperature conditions are not entirely accurate as they were obtained using correlations and not measured directly, which can be a source of error.

			0.5 M Acetic acid		1.0 M Acetic acid	
			Experimental Results	Fredd and Fogler Method	Experimental Results	Fredd and Fogler Method
RPM	ω	ω^1/2	Dissolution rate	Dissolution Rate	Dissolution rate	Dissolution Rate
100	10.46667	3.235223	1.33E-07	1.00E-07	2.67E-07	1.20E-07
300	31.4	5.60357	2.69E-07	1.90E-07	3.99E-07	2.20E-07
500	52.33333	7.234178	2.24E-07	2.00E-07	4.96E-07	2.80E-07
1000	104.6667	10.23067	4.43E-07	2.80E-07	6.43E-07	3.80E-07
1300	136.0667	11.66476	5.90E-07	3.50E-07	6.70E-07	4.00E-07
1500	157	12.52996	5.22E-07	3.80E-07	8.15E-07	4.40E-07

Table 5.1: Comparative analysis: Experimental and Fredd and Fogler Results

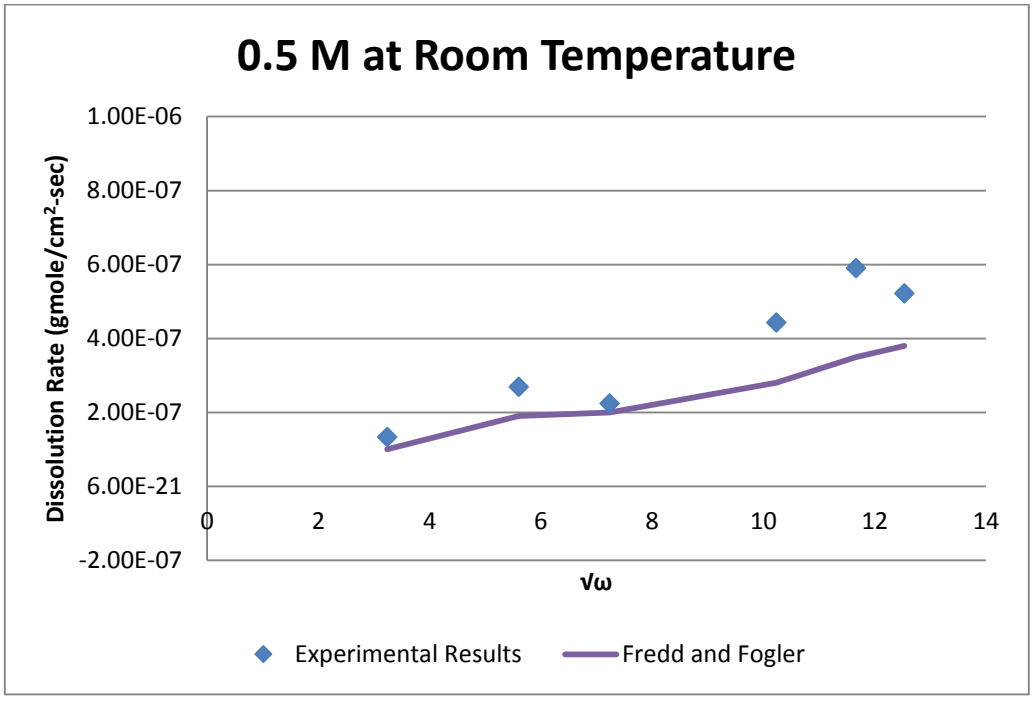

Figure 5.1: 0.5 M Acetic acid at room temperature

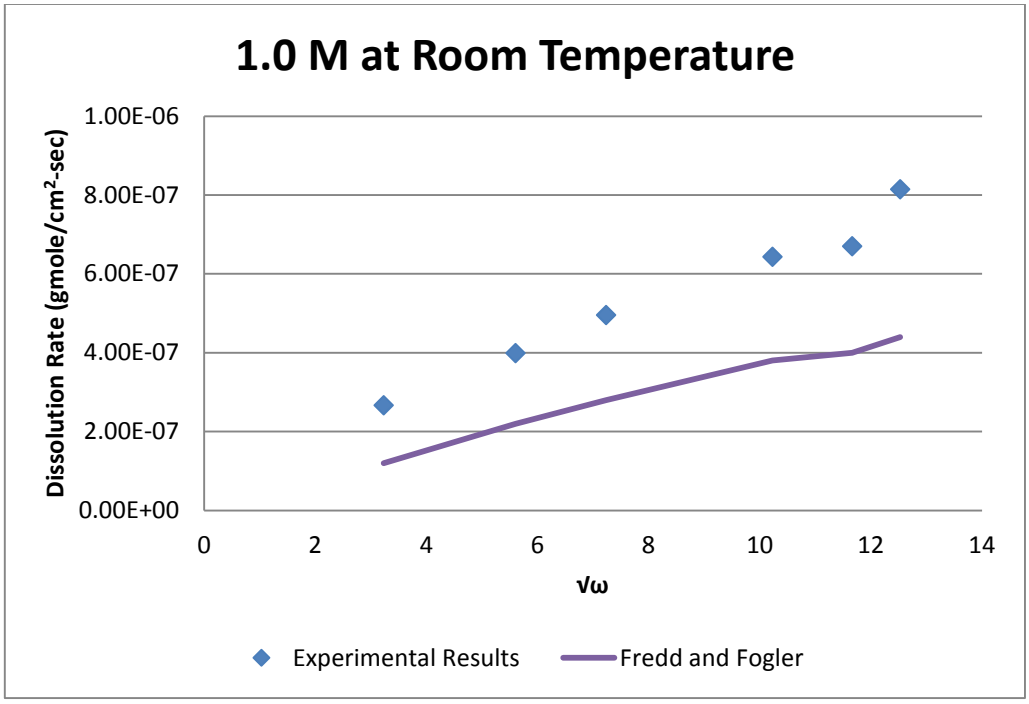

Figure 5.2: 1.0 M acetic acid at room temperature

Additional results in the form of effective forward reaction rate constant (k_r), effective equilibrium constant (K_{eff}), and contribution of each of the three reaction steps at room temperature were also obtained and these values are compared to the published data (Table 5.2).

	Concentration	k_r (cm/s)	K_{eff}	Reactant Transport	Surface Reaction	Product Transport
Published Results	**0.5 M**	5.00E-03	0.16	18.00	16.00	66.00
Model Results		3.47E-03	0.259	14.60	7.68	77.72
Published Results	**1.0 M**	2.00E-03	0.087	11.00	15.00	74.00
Model Results		3.91E-03	0.171	10.25	6.83	82.92

Table 5.2: Overall comparison with Fredd and Fogler method

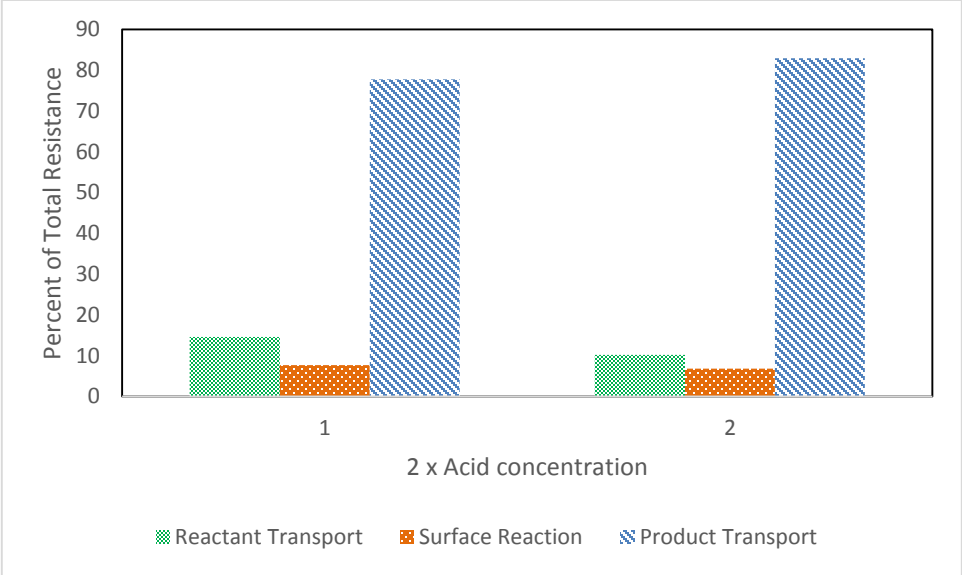

Figure 5.3: Resistance contribution of each reaction step

From Fig. 5.3, it can be observed that the mass transfer process of reactants and products have a very high impact on the overall reaction kinetics and it increases with increase in initial acid concentration. The contribution of surface reaction is also significant and should not be considered negligible.

Buijse et al. (2004) approach is much simpler and straight forward. This model considers that all the different types of acids react with calcite in a similar manner and the only variation in the reaction rate result arises due to the difference in the degrees of acid dissociation of these acid solutions. The rate calculation steps by this approach is described through an algorithm shown in Fig. 5.4.

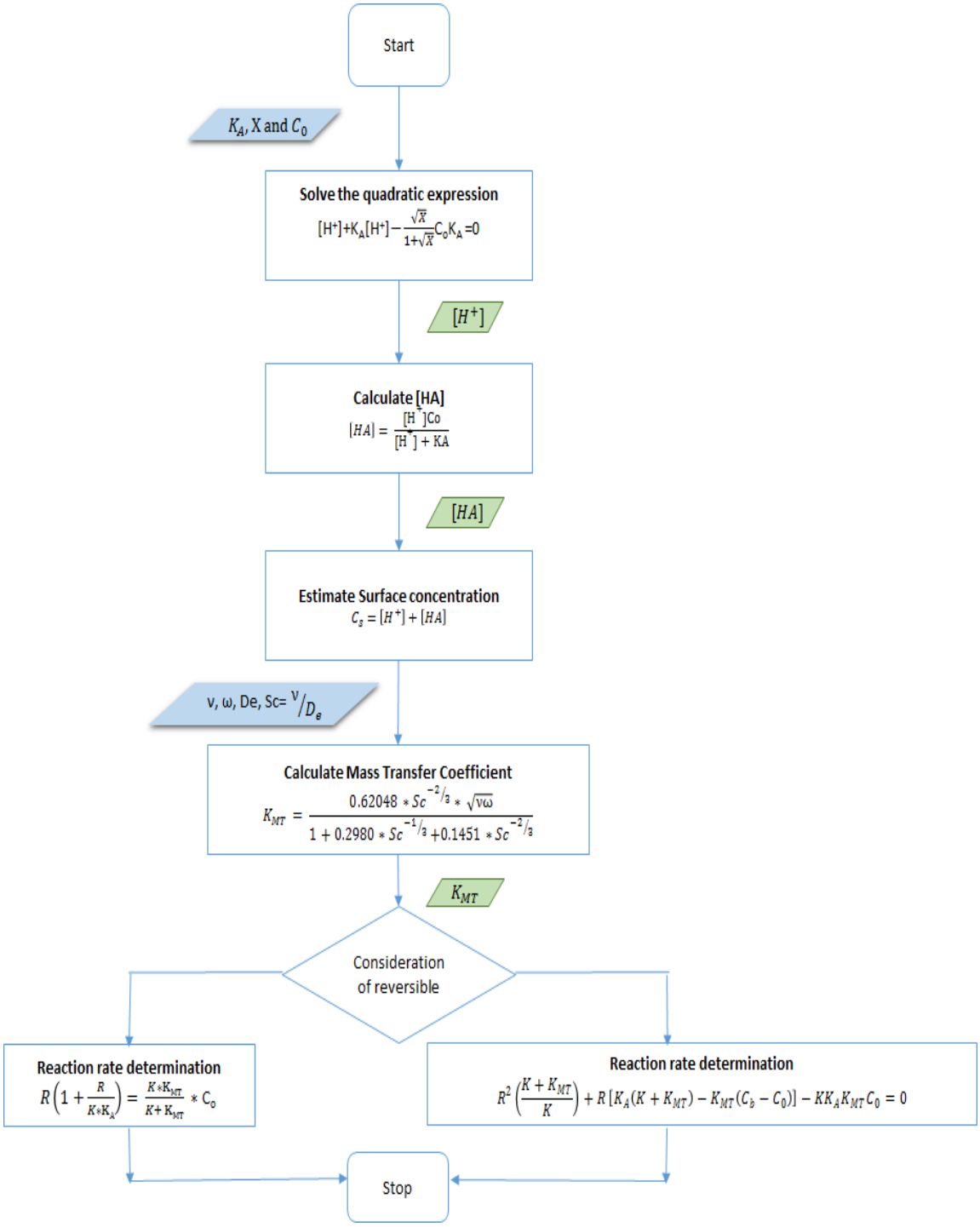

Figure 5.4: Algorithm - Buijse et al. approach

It can be inferred from the Fig 5.4 that there are two distinct ways to determine the reaction rates, viz. by considering the effect of reversible reaction or by ignoring it. An excel program (As shown in the appendix) was developed on the basis of this algorithm and reaction rates were estimated at all the experimental conditions. A sample comparison for 1.5 M acetic acid solution at room temperature is included in Table 5.3.

	RPM	ω	ω^1/2	Experimental Dissolution rate	Without backward reactions	With backward reactions
1.5 M Acetic acid	100	10.46667	**3.235223**	**2.97E-07**	8.54E-07	3.76E-07
	300	31.4	**5.60357**	**3.96E-07**	1.14E-06	4.16E-07
	500	52.33333	**7.234178**	**3.81E-07**	1.29E-06	4.32E-07
	700	73.26667	**8.559595**	**4.24E-07**	1.39E-06	4.41E-07
	1000	104.6667	**10.23067**	**4.25E-07**	1.51E-06	4.49E-07
	1300	136.0667	**11.66476**	**5.22E-07**	1.60E-06	4.54E-07
	1500	157	**12.52996**	**6.22E-07**	1.65E-06	4.57E-07

Table 5.3: Comparative analysis: Experimental and Buijse method

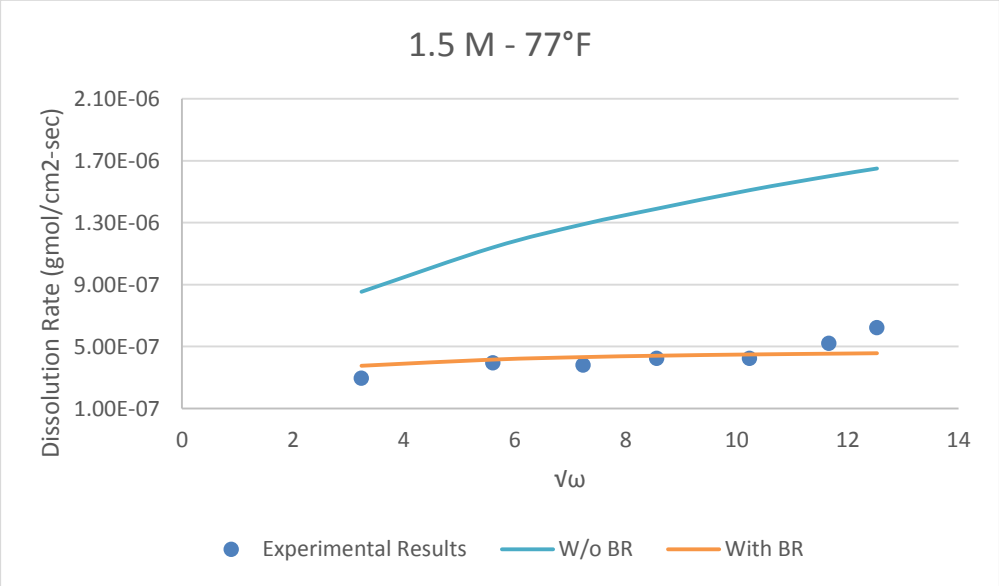

Figure 5.5: 1.5 M acid at room temperature

At room temperature, the surface reaction effect is very dominant and therefore, we observe that the reaction rates calculated by considering the reversible reaction effect agrees very well with the experimental values as shown in Fig. 5.5. The same trend was followed by other acid solutions at room temperature as well. In order to analyze the temperature effect on the reaction rate determination process, we carried out the similar experiments at elevated temperature (150 and 200°F). The kinematic viscosity and diffusion coefficient were corrected for the temperature increment and the updated values were used in the model. The comparative results for these two conditions are described in Fig. 5.6 and Fig. 5.7.

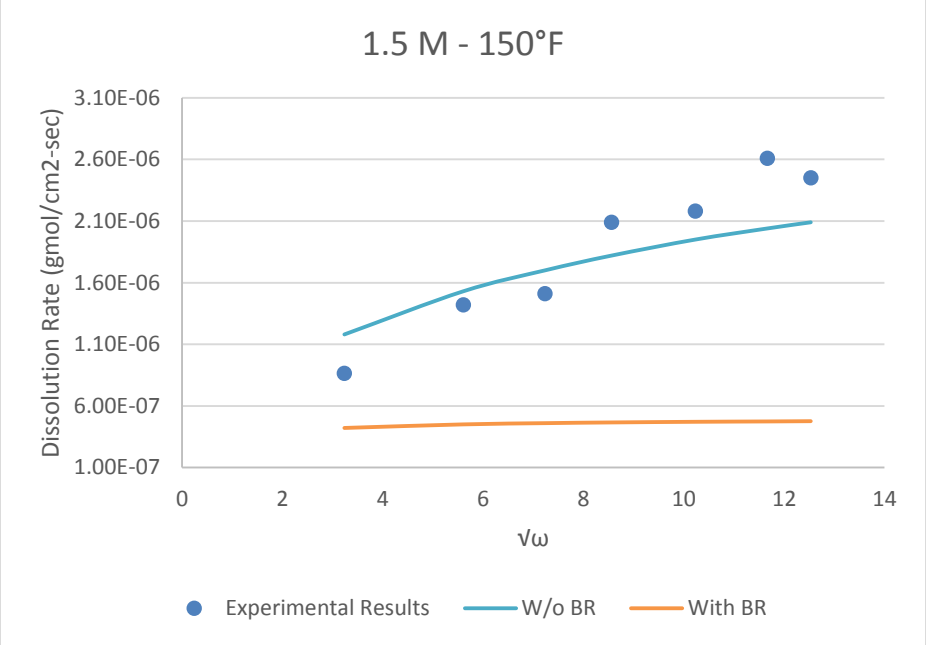

Figure 5.6: 1.5 M acid at 150°F

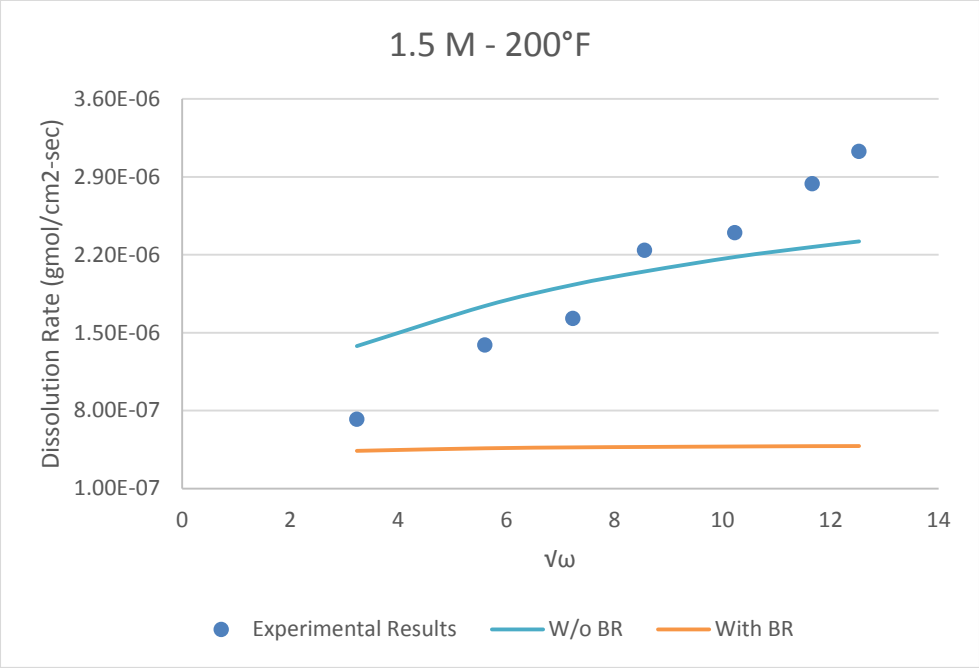

Figure 5.7: 1.5 M acid at 200°F

A clear difference between these two cases can be seen as compared to the room temperature results. For elevated temperature conditions, the acid reactivity increases thus driving the overall reaction in the forward direction. The impact of reversible reaction decreases with temperature increment and hence the model results estimated by neglecting the reversible reactions are coherent with the experimental results at higher temperatures.

CHAPTER VI

APPLICATION AND CONCLUSIONS

Acidizing a damaged formation using HCl is an efficient and cost effective method but at high temperature conditions, it is associated with various drawbacks such as rapid rock dissolution, high corrosion rate, sludge formation tendency with asphaltene molecules, etc. Different organic acid solutions like formic, acetic and citric acid are used as an alternative to HCl for higher temperature acidizing jobs. These acid solutions have shown good field applications but they too have certain limitations which hinders its performance as stimulation fluid. Firstly, these acids are weakly dissociated and therefore have lower reactivity compared to HCl. Formic acid is among the strong organic acids and still its dissociation constant in just about 1.3%. Apart from this the reaction between formic acid and calcite generates calcium formate, which has very low solubility at higher concentrations. Furthermore, the use of formic acid also causes many environmental issues. Acetic acid also showcases some of the aforementioned limitations, but in a very low magnitude and therefore is used most widely. Although the application of acetic acid in the field of acidizing started even before 1960, its reaction kinetics is not comprehensively studied. The impact of backward reactions on the overall reaction rate determination lacks clarity.

The focus of this study was to look into the effect of reversible reactions on the overall kinetics of the acidizing process involving organic acids. Acetic acid was chosen as a representative organic acid and all the analysis were carried out using its different

concentration solutions. The reaction of acetic acid with calcite is known to be thermodynamically limited by the presence of products at the reaction surface. Study conducted by Buijse et al. (2004) highlighted that for pH values lower than 4, the effect of reversible reactions on the overall rate determination process is negligible and can be neglected. This means that the acidizing process of acetic acid can be modeled in the same way as HCl, which works on the principle of complete dissociation and does not incorporate impact of partial dissociation.

In this study, different models were developed on the basis of earlier research and rotating disk experiments were carried out at various conditions to establish the effectiveness of the theoretical models. Using Fredd and Fogler (1998) approach, the activation energy value required to complete the acetic acid reaction with calcite was calculated. A comparison of the calculated value with that obtained for a purely diffusion limited process showed that additional activation energy is required to complete the process due to occurrence of reversible reactions. In addition to determination of activation energy, this model was also used to evaluate the contribution of each of the mass transfer as well as the surface reaction process on the overall reaction resistance. It was inferred that the mass transport of products away from the surface had maximum contribution to the overall resistance, followed by the mass transfer of reactants. The surface reaction process also had considerable contribution and hence should not be neglected. The experimental results also agreed with the theoretically calculated results from the model.

Another model on the basis of the work published by Buijse et al. (2004) was developed and used to estimate the reaction rate values at different acid concentration and temperature conditions. The calculated results showed coherence with the experimental results, thus validating it. Two approaches were included while developing this model, one of them considered the effect of reversible reaction on the rate determination step while the other did not. It was observed that at lower temperature conditions, the experimental data matched the former approach describing the effect of reversible reaction. Contrarily, as the temperature is increased, the impact of the backward reaction reduces as the reactivity of the acid increases. This results in a better match of experimental data with the latter approach where reversible reactions are neglected at higher temperature condition.

Important inferences derived from this work is that the occurrence of reversible reactions causes increase in the activation energy of the process by a considerable degree and therefore its significance should not be neglected. Secondly, increase in temperature enhances the acid reactivity and decreases the effect of reversible reactions and therefore at high temperature conditions, reaction rate modeling without considering the effect of backward reactions can give appropriate results.

CHAPTER VII

FUTURE WORK

The work presented in this research describes the reaction kinetics of acetic acid with calcite and focuses on the impact that reversible reactions have on the overall rate of reaction. Additional experimental work including a complete set of rotating disk experiments for other organic acids at different temperatures and acid concentrations should be conducted. The results obtained from RDA experiments could be used in the model to estimate various kinetic and mass transfer parameters. Moreover, the effect of other additives that are added to prepare an acid solution on the overall reaction rate could also be studied.

The optimum acid injection rate could also be evaluated by performing a set of core-flood experiments for different initial acid concentration at various temperature conditions.

REFERENCES

Bennion, D.B., Thomas F.B. 1994. Underbalanced Drilling of Horizontal Wells : Does It Really Eliminate Formation Damage?. International Symposium of Formation Damage Control, Lafayette, Louisiana. http://dx.doi.org/10.2118/27352-MS.

Boomer, D.R., McCune, C.C., Fogler, H.S. 1972. Rotating Disk Apparatus for Reaction Rate Studies in Corrosive Liquid Environments. *Review of Scientific Instruments* **43** (2): 225-229. http://dx.doi.org/10.1063/1.1685599.

Buijse, M., de Boer, P., Breukel, B. et al. 2004. Organic Acids in Carbonate Acidizing. *SPE Production and Facilities* **19** (3): 128-134. http://dx.doi.org/10.2118/82211-PA.

Callen, H.B. 1985. *Thermodynamics and an Introduction to Thermostatics*. Singapore, Wiley (Reprint).

Chatelain, J.C., Silberberg I.H., Schechter R.S. 1976. Thermodynamic Limitations in Organic-Acid / Carbonate Systems, *SPE J.* **16** (4): 189-195. http://dx.doi.org/10.2118/5647-PA.

Crowe, C.W., Minor, S.S. 1982. Acid Corrosion Inhibitor Adsorption and its Effect on Matrix Stimulation Results. SPE Formation Damage Control Symposium, Lafayette, Louisiana. http://dx.doi.org/10.2118/10650-MS.

Davies, C.W. 1962. *Ion Association*. Washington, Buttersworths (Reprint).

Ellison, B.T., Cornet I. 1971. Mass Transfer to a Rotating Disk. *J. Electrochemical Society* **118** (1): 68-72. http://dx.doi.org/10.1149/1.2407954.

Fredd, C.N., Fogler, H.S. 1998. Alternative Stimulation Fluids and Their Impact on Carbonate Acidizing. *SPE J.* **3** (1): 34–41. http://dx.doi.org/10.2118/31074-PA.

Fredd, C.N., Fogler, H.S. 1998. The Kinetics of Calcite Dissolution in Acetic Acid Solutions. *Chemical Engineering Science* **53** (22): 3863-3874. http://dx.doi.org/10.1016/S0009-2509(98)00192-4.

Gregory, D.P., Riddiford, A.C. 1956. Transport to the Surface of a Rotating Disc. *J. Chem. Soc.* **6**: 3756–3764. http://dx.doi.org/10.1039/jr9560003756.

Harned, H.S., Owen, B.B. 1958. *The Physical Chemistry of Electrolytic Solutions*. New York: Reinhold. (Reprint).

Harris, F.N. 1961. Applications of Acetic Acid to Well Completion, Stimulation and Reconditioning. *J. Pet. Tech.* **13** (7): 637–639. http://dx.doi.org/10.2118/63-PA.

Hou, X., Jones, B. T. 2008. Inductively Coupled Plasma - Optical Emission Spectrometry. *Encyclopedia of Analytical Chemistry*: pp. 9468-9485. http://dx.doi.org/10.1002/9780470027318.a5110.

Kalfayan, L. 2008. *Production Enhancement with Acid Stimulation*. Tulsa, Oklahoma. PennWell (Reprint).

Levich, V.G. 1962. *Physiochemical Hydrodnamics*. New Jersey, Englewood Cliffs, Prentice Hall (Reprint).

Litt, M., Serad G. 1964. Chemical Reactions on a Rotating Disk. *Chemical Engineering Science* **19**: 867–884. http://dx.doi.org/10.1016/0009-2509(64)85065-X.

Lund, K., Fogler, H.S., McCune, C.C., Ault, J.W. 1975. Acidization - I. The Dissolution of Dolomite in Hydrochloric Acid. *Chemical Engineering Science* **28** (3): 691,IN1 – 700, IN1. http://dx.doi.org/10.1016/0009-2509(77)80003-1.

Lund, K., Fogler, H.S., McCune, C.C. 1973. Acidization - II. The Dissolution of Calcite in Hydrochloric Acid. *Chemical Engineering Science* **30** (8): 825–835. http://dx.doi.org/10.1016/0009-2509(75)80047-9.

Nancollas, G.H. 1956. Thermodynamics of Ion Association, Part II — Alkaline-earth Acetates and Formates. *J. Chem. Soc*.: 744 – 749. http://dx.doi.ogr/10.1039/JR9560000744.

Newman, J. 1966. Schmidt Number Correction for the Rotating Disk. *The Journal of Physical Chemistry* **70** (4): 1327–28. http://dx.doi.org/10.1021/j100876a509.

Nierode, D.E., Williams, B.B. 1971. Characteristics of Acid Reaction in Limestone Formations. *SPE J.* **11** (4): 406 – 418. http://dx.doi.org/10.2118/3101-PA.

Plummer, L.N., Wigley, T.M.L., Parakhurst, D.L. 1978. The Kinetics of Calcite Dissolution in CO_2 Water Systems at 5° to 60° C and 0.0 to 1.0 atm CO_2. *American Journal of Science* **278** (2): 179-216. http://dx.doi.org/10.2475/ajs.278.2.179.

Pokrovsky, O.S., Golubev, S.V., Schott, J. 2005. Dissolution Kinetics of Calcite, Dolomite and Magnesite at 25 °C and 0 to 50 atm pCO_2. *Chemical Geology* **217** (3-4): 239–255. http://dx.doi.org/10.1016/j.chemgeo.2004.12.012.

Rabie, A.I., Shedd, D.C., Nasr-El-din, H.A. 2014. Measuring the Reaction Rate of Lactic Acid with Calcite and Dolomite by Use of the Rotating-Disk Apparatus. *SPE J* **19** (6): 1192-1202. http://dx.doi.org/10.2118/140167-PA.

Robinson, R.A., Stokes, R.H. 1955. *Electrolyte Solutions: The Measurement and Interpretation of Conductance, Chemical Potential and Diffusion in Solutions of Simple Electrolytes*. London, Buttersworths (Reprint).

Rozieres, J., Chang, F.F., Sullivan, R.B. 1994. Measuring Diffusion Coefficients in Acid Fracturing Fluids and Their Application to Gelled and Emulsified Acids. SPE Annual Technical Conference and Exhibition, New Orleans, Louisiana. http://dx.doi.org/10.2118/28552-MS.

Schauhoff, S.N., Kissel, C.L. 2000. New Corrosion Inhibitors for High Temperature Applications. *Materials and Corrosion* **51** (3): 141-146. http://dx.doi.org/10.1002/(SICI)1521-4176(200003)51:3<141::AID-MACO141>3.0.CO;2-N.

Schechter, R.S. 1992. *Oil Well Stimulation*. Englewood Cliff, New Jersey: Prentice Hall Inc. (Reprint).

Schlichting, H. 1960. *Boundary-layer Theory*. New York: McGraw-Hill (Reprint).

Sjöberg, E.L., Rickard, D.T. 1984. Calcite Dissolution Kinetics: Surface Speciation and the Origin of the Variable pH Dependence. *Chemical Geology* **42** (1-4): 119-136. http://dx.doi.org/10.1016/0009-2541(84)90009-3.

Taylor, K.C., Nasr-El-Din, H.A. 2009. Measurement of Acid Reaction Rates with the Rotating Disk Apparatus. *Journal of Canadian Petroleum Technology* **48** (6): 66-70. http://dx.doi.org/10.2118/09-06-66.

Truesdell, A.H., Jones, B.F. 1974. WATEQ, A Computer Program for Calculating Chemical Equilibria of Natural Waters. *Journal of Research of the U.S. Geological Survey* **2** (2): 233-248.

Williams, B.B., Gidley, J.L., Schechter, R.S. 1979. *Acidizing Fundamentals*. New York: Henry L. Doherty Memorial Fund of AIME (Reprint).

Vitagliano, V., Lyons, P.A. 1956. Diffusion in Aqueous Acetic Acid Solutions. *Journal of the American Chemical Society* **78** (18): 4538–4542. http://dx.doi.org/10.1021/ja01599a008.

APPENDIX

Excel Program - Buijse et al. Model

Reaction Rate Calculations

Co	0.5	mol/L	v	0.926	centi-stokes	K	0.023
	0.0005	mol/cm3		0.00926	cm2/sec	n	0.6
Ka	1.7378E-05		ω	100	rpm	K2	2.50E-04
X	1.94E-10			10.46666667	rad/s		
			De	1.13E-05	cm2/sec		
Temperature (F)	77					K1	600
						K3	5.60E-11
At equilibrium			**Mass Transfer Parameters**			Ksp	3.00E-08
a	1		√νω	0.311321913			
b	1.7378E-05		Sc	8.23E+02			
c	-1.21E-13						
[H]	6.96927E-09	-1.7385E-05	Numerator	0.002194455			
[HA]	2.0044E-07		Denominator	1.03E+00			
Ceq	2.07409E-07		Kmt	2.12E-03			
Spent fraction	0.999585182						
Unspent fraction	0.000414818						
At surface							Input Variables
							Intermediate Calculations
Acid strength	0.00417						Co-efficients of quadratic equation
[H]	1.72979E-06						Reaction Rate
[HA]	4.5264E-05						
Cs	4.69938E-05						
Rate without considering BR			**Rate BR consideration**				
a	2501912.771		a	1.092316969		8.02646E-06	
b	1		b	1.40E-06		-3.4722E-05	
c	-9.7192E-07		c	-4.24E-13			
R w/o BR	4.54683E-07	-8.54377E-07	R with BR	2.5331E-07	-1.53358E-06		

Room Temperature

0.5 M Acetic acid

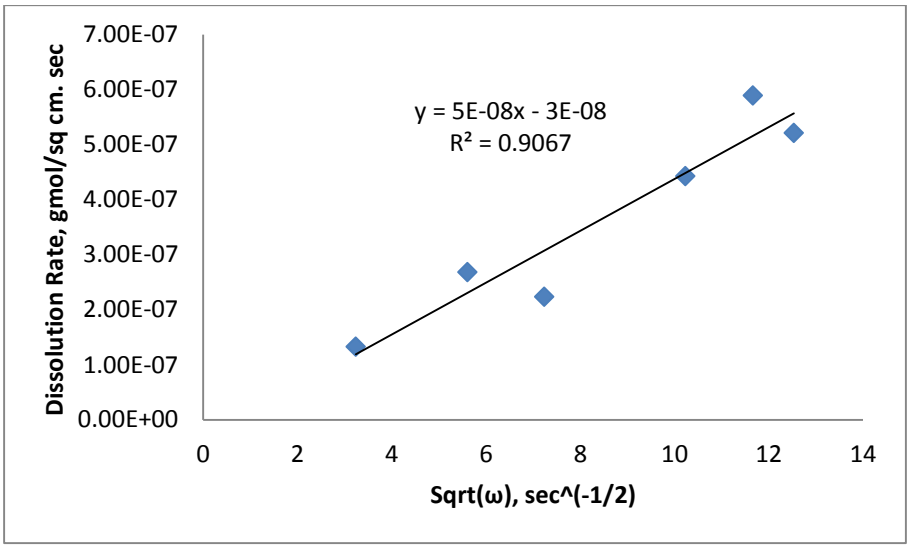

1.0 M Acetic acid

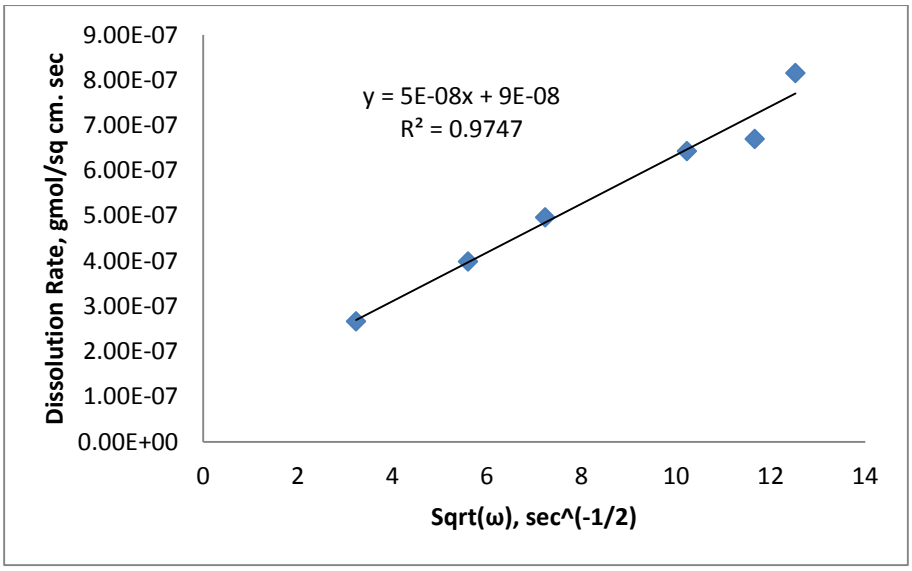

1.5 M Acetic acid

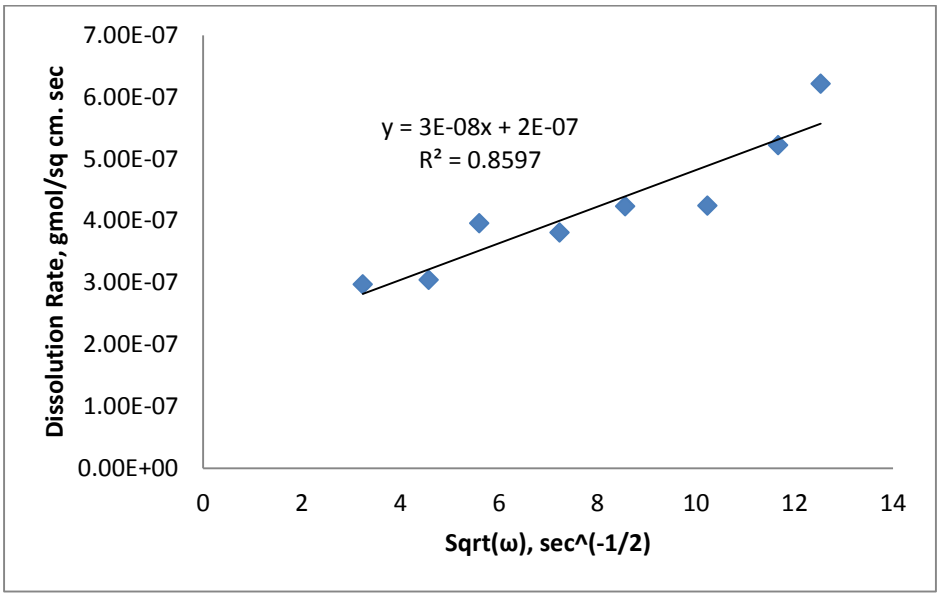

2.0 M Acetic acid

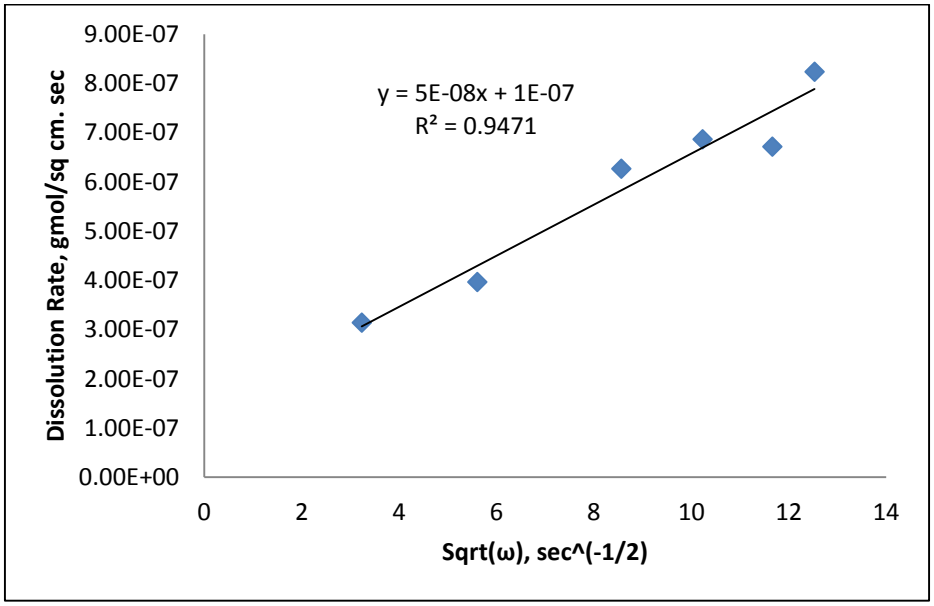

150°F

0.5 M Acetic acid

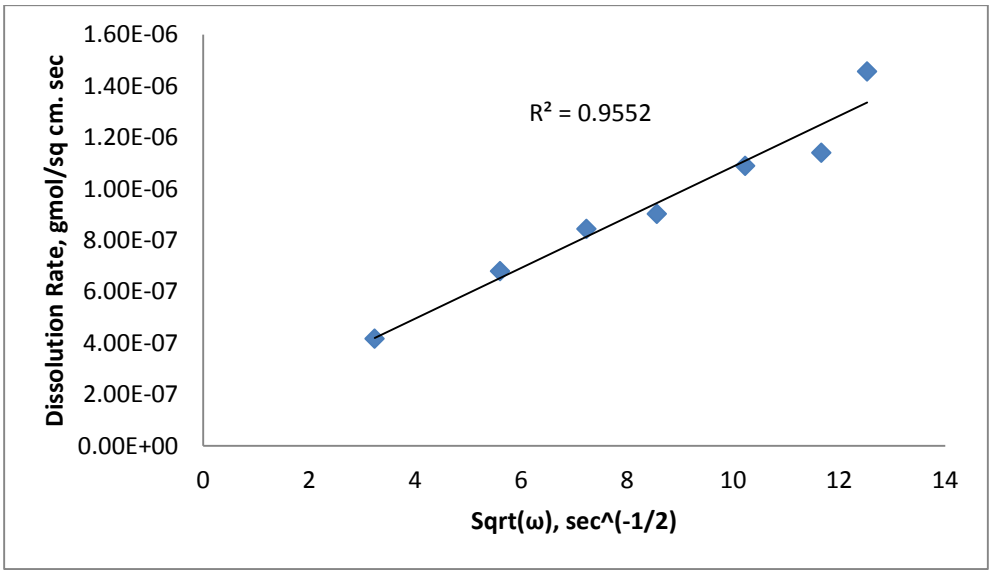

1.0 M Acetic acid

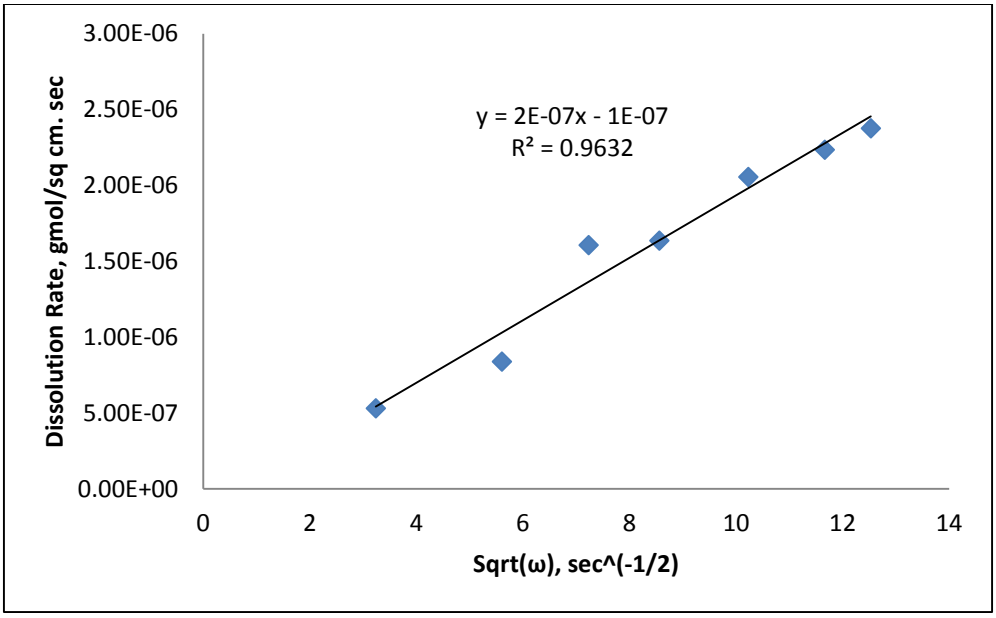

1.5 M Acetic acid

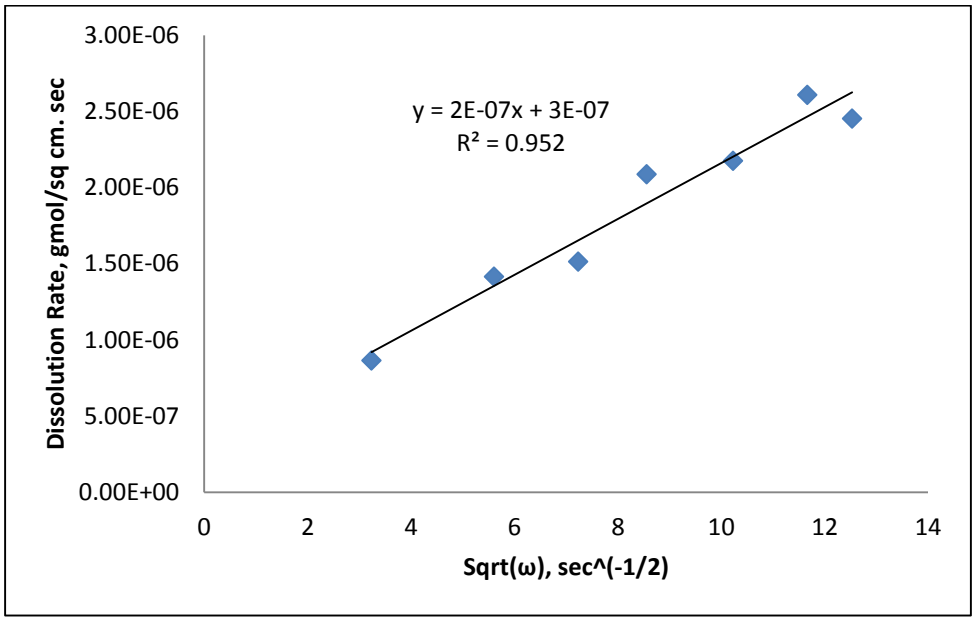

2.0 M Acetic acid

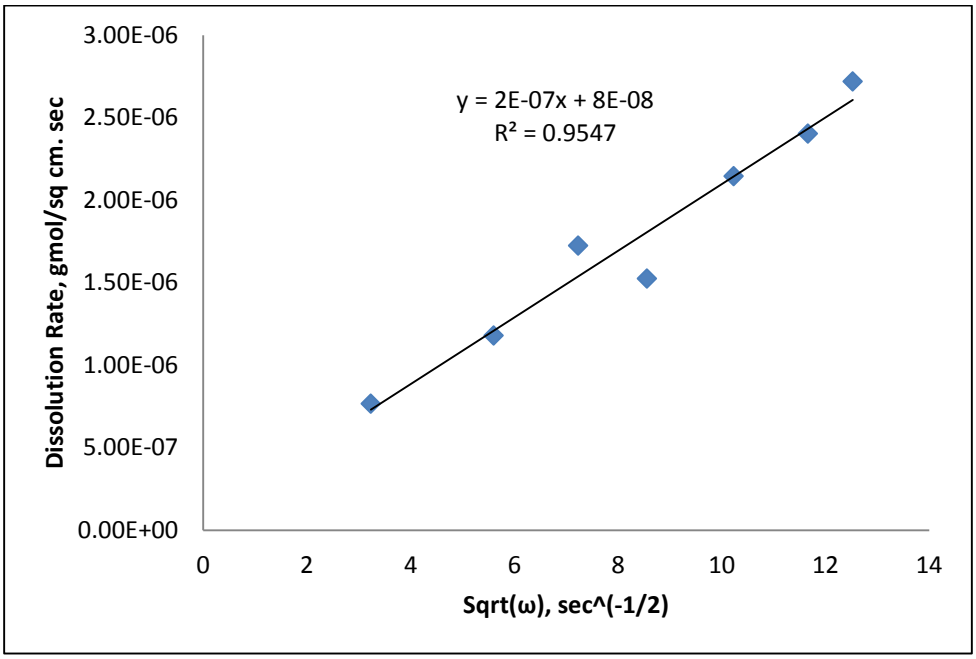

200°F

0.5 M Acetic acid

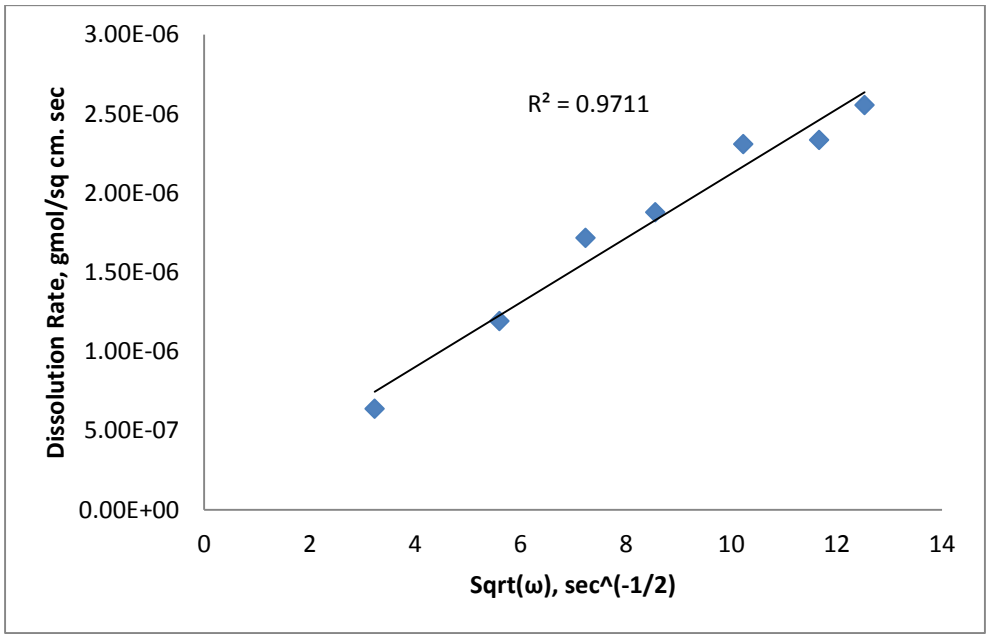

1.0 M Acetic acid

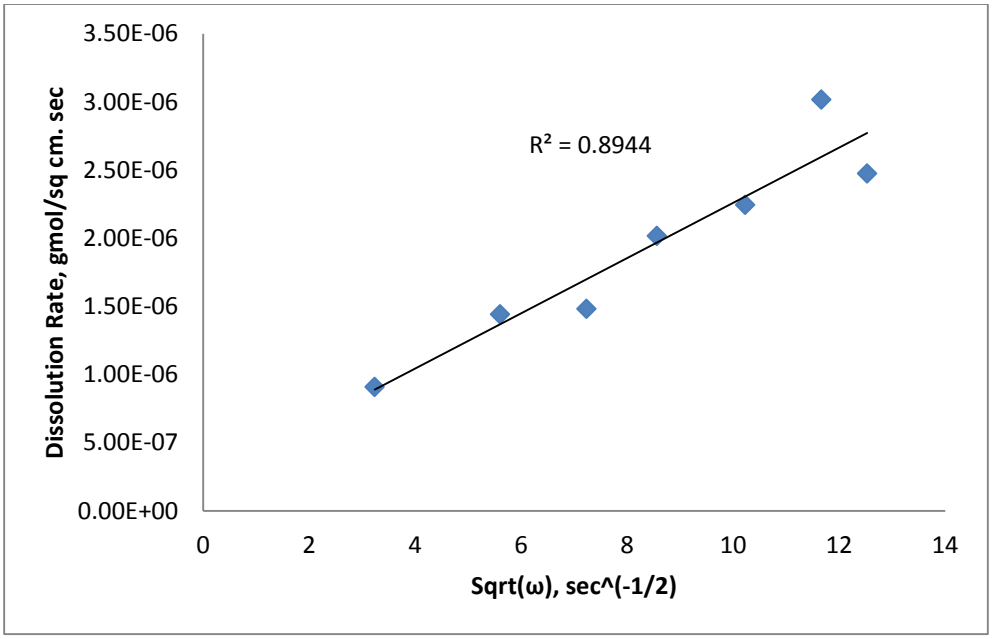

1.5 M Acetic acid

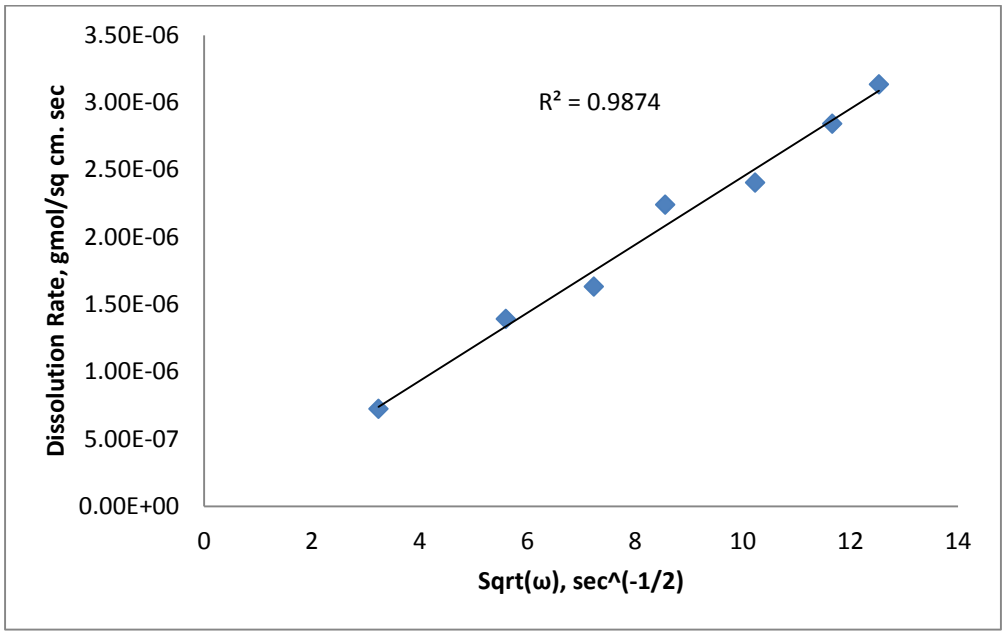

2.0 M Acetic acid

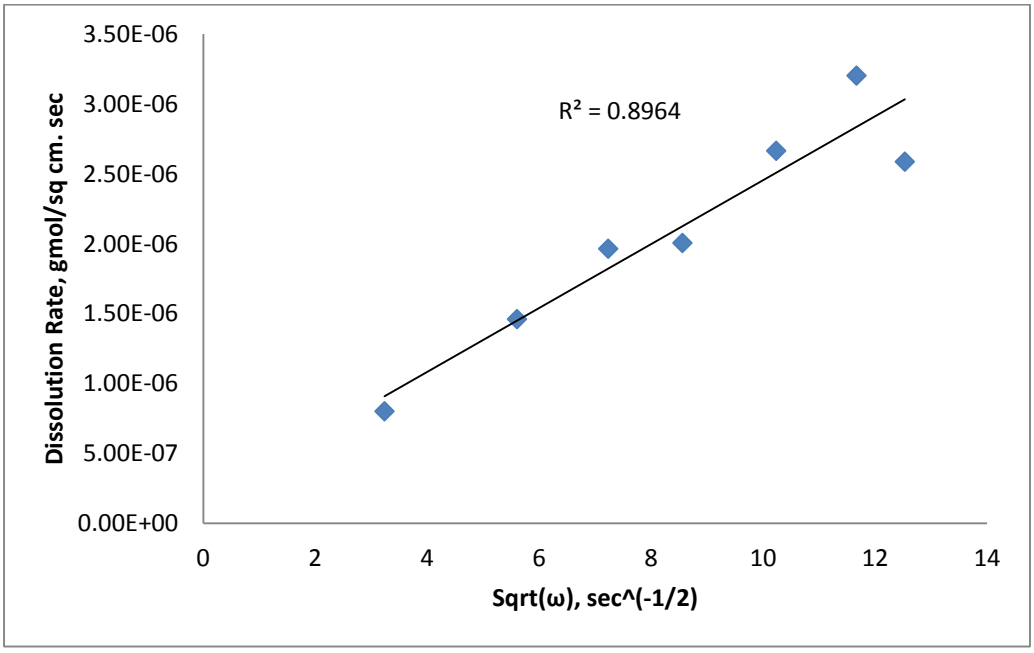

Rotating Disk Experiments

	Room Tempearture				150 F				200 F			
0.5 M Acetic acid	RPM	ω	ω^1/2	Dissolution rate	RPM	ω	ω^1/2	Dissolution rate	RPM	ω	ω^1/2	Dissolution rate
	100	10.46667	3.235223	1.33E-07	100	10.46667	3.235223	4.17E-07	100	10.46667	3.235223	6.38E-07
	300	31.4	5.60357	2.69E-07	300	31.4	5.60357	6.80E-07	300	31.4	5.60357	1.19E-06
	500	52.33333	7.234178	2.24E-07	500	52.33333	7.234178	8.44E-07	500	52.33333	7.234178	1.72E-06
	1000	104.6667	10.23067	4.43E-07	700	73.26667	8.559595	9.03E-07	700	73.26667	8.559595	1.88E-06
	1300	136.0667	11.66476	5.90E-07	1000	104.6667	10.23067	1.09E-06	1000	104.6667	10.23067	2.31E-06
	1500	157	12.52996	5.22E-07	1300	136.0667	11.66476	1.14E-06	1300	136.0667	11.66476	2.34E-06
					1500	157	12.52996	1.46E-06	1500	157	12.52996	2.56E-06
1.0 M Acetic acid	RPM	ω	ω^1/2	Dissolution rate	RPM	ω	ω^1/2	Dissolution rate	RPM	ω	ω^1/2	Dissolution rate
	100	10.46667	3.235223	2.67E-07	100	10.46667	3.235223	5.31E-07	100	10.46667	3.235223	9.11E-07
	300	31.4	5.60357	3.99E-07	300	31.4	5.60357	8.40E-07	300	31.4	5.60357	1.44E-06
	500	52.33333	7.234178	4.96E-07	500	52.33333	7.234178	1.61E-06	500	52.33333	7.234178	1.48E-06
	1000	104.6667	10.23067	6.43E-07	700	73.26667	8.559595	1.64E-06	700	73.26667	8.559595	2.02E-06
	1300	136.0667	11.66476	6.70E-07	1000	104.6667	10.23067	2.06E-06	1000	104.6667	10.23067	2.25E-06
	1500	157	12.52996	8.15E-07	1300	136.0667	11.66476	2.24E-06	1300	136.0667	11.66476	3.02E-06
					1500	157	12.52996	2.38E-06	1500	157	12.52996	2.98E-06
1.5 M Acetic acid	RPM	ω	ω^1/2	Dissolution rate	RPM	ω	ω^1/2	Dissolution rate	RPM	ω	ω^1/2	Dissolution rate
	100	10.46667	3.235223	2.97E-07	100	10.46667	3.235223	8.65E-07	100	10.46667	3.235223	7.24E-07
	200	20.93333	4.575296	3.04E-07	300	31.4	5.60357	1.42E-06	300	31.4	5.60357	1.39E-06
	300	31.4	5.60357	3.96E-07	500	52.33333	7.234178	1.51E-06	500	52.33333	7.234178	1.63E-06
	500	52.33333	7.234178	3.81E-07	700	73.26667	8.559595	2.09E-06	700	73.26667	8.559595	2.24E-06
	700	73.26667	8.559595	4.24E-07	1000	104.6667	10.23067	2.18E-06	1000	104.6667	10.23067	2.40E-06
	1000	104.6667	10.23067	4.25E-07	1300	136.0667	11.66476	2.61E-06	1300	136.0667	11.66476	2.84E-06
	1300	136.0667	11.66476	5.22E-07	1500	157	12.52996	2.45E-06	1500	157	12.52996	3.13E-06
	1500	157	12.52996	6.22E-07								
2.0 M Acetic acid	RPM	ω	ω^1/2	Dissolution rate	RPM	ω	ω^1/2	Dissolution rate	RPM	ω	ω^1/2	Dissolution rate
	100	10.46667	3.235223	3.14E-07	100	10.46667	3.235223	7.67E-07	100	10.46667	3.235223	8.00E-07
	300	31.4	5.60357	3.97E-07	300	31.4	5.60357	1.18E-06	300	31.4	5.60357	1.46E-06
	500	52.33333	7.234178	4.53E-07	500	52.33333	7.234178	1.73E-06	500	52.33333	7.234178	1.96E-06
	700	73.26667	8.559595	6.27E-07	700	73.26667	8.559595	1.52E-06	700	73.26667	8.559595	2.01E-06
	1000	104.6667	10.23067	6.86E-07	1000	104.6667	10.23067	2.15E-06	1000	104.6667	10.23067	2.67E-06
	1300	136.0667	11.66476	6.72E-07	1300	136.0667	11.66476	2.40E-06	1300	136.0667	11.66476	3.20E-06
	1500	157	12.52996	8.24E-07	1500	157	12.52996	2.72E-06	1500	157	12.52996	2.59E-06